scientific reports

Check for updates

OPEN

Divergent features of collective gravitational quantum excitations

M. Akbari-Moghanjoughi

In this research, we study different aspects of collective gravitational quantum excitations in the framework of the quantum multistream model. The energy dispersion of collective electrostatic (plasmon) and gravitational excitations or as we call gravity quasiparticle (GQ) are derived using the nonrelativistic and relativistic models and many parameters such as the effective mass, phase, and group speed of quasiparticle excitations are studied, in detail. It is shown that, unlike plasmons with a forbidden energy gap, all positive and negative energy values are allowed for GQs. However, unlike plasmon with a dual-tone nature of collective excitations, the GQs are found to be single-tone with either wave-like or particle-like oscillations being strongly damped. The linear phase-space evolution of GQs indicates that they evolve similarly to the classical system of particles in the center of the mass frame in which the force due to self-consistent gravitational potential plays the role of interparticle forces. It is shown that the damping of wavelike or particle-like excitations in GQ energy dispersion leads to three distinct phenomena of gravitational expansion ($E > 0$), stable matter ($E = 0$) and gravitational collapse ($E < 0$), respectively. The Hubble-Lemaitre-like relation is obtained from the generalized probability current for GQs. The quantum gravitational interference effect is also studied.

Gravity is a fundamental force of nature with a relatively less understood quantum features regarding other forces governing the universe. Because of the very large-scale characteristics of gravity, physical theories confront a major hierarchy problem leading to huge discrepancies between aspects of the weak force and gravity. No evidence has yet been found to explain why gravity which governs the large-scale effects of the universe is at least 29 orders of magnitude weaker than the weakest force of nature and 39 orders of magnitude smaller than the strong nuclear force. The hierarchy problem is known as the main cause of failure in renormalization[1] of gravity in quantum field theories via the coupling constant in unification attempts. The hierarchy problem is also closely related to the naturalness and fine-tuning models of nature. To circumvent the hierarchy problem Arkani-Hamed, Dimopoulos, and Dvali proposed the ADD model in 1998[2] to attribute the weakness of gravity to the existence of extra-large dimensions assuming that while the known fields of the standard model are confined to our four-dimensional membrane, gravity acts as a multidimensional force in other dimensions large compared to the Planck scale. However, no experimental evidence of the existence of extra-large dimensions has been reported yet and the results of the Large Hadron Collider (LHC) strongly contrast the theories of such predictions[3]. Randall-Sundrum models, on the other hand, try to solve the hierarchy problem using an alternative compactification[4] by describing the physical world in terms of warped-geometry higher-dimensional universe in which elementary particles are localized in a $(3+1)$-dimensional brane[5]. Another element of the hierarchy problem is the so-called cosmological constant[6] problem in which a tiny nonzero constant appears in general relativity formulation in an *ad hoc* manner to account for the accelerating universe. This constant was first introduced by Einstein himself to maintain a static universe but later removed after the confirmation of the expanding universe by observations of Edwin Hubble[7]. The modern cosmological constant is closely related to the concept of dark energy[8].

More than a century after the emergence of two overwhelming modern physics theories, namely quantum mechanics and general relativity, a self-consistent theory of quantum gravity is still out of reach. The most basic question of why these extremely successful theories cannot be combined in a single theory of quantum gravity turns out to be among the hardest questions in all the history of physics. Quantum gravity is a field of research where quantum and gravitational effects are supposed to be equally important. Exploration of fundamental aspects of our universe, such as its nontrivial existence and evolution, the nature of black hole singularities, and the state of matter in extremely dense astrophysical objects like neutron stars strongly relies on a unified picture of quantum and gravity. One of the biggest obstacles encountered in developing such a theory is that its experimental verification requires extremely high energies which appear to be near the Planck length scale of the order of 10^{-35} meters or smaller which is not in the accessible range of currently operating high energy particle accelerators. Therefore, physicists are forced to use their imaginations as thought experiments besides

Department of Physics, Faculty of Sciences, Azarbaijan Shahid Madani University, 51745-406, Tabriz, Iran. email: massoud2002@yahoo.com

pursuing the mathematical beauty and inherent symmetries of nature. However, new trends to observe effects at the Planck lengthscales based on the matter waves decoherence and search for violation of quantum mechanics has been previously proposed[9,10]. The list of theories seeking to incorporate gravity into quantum mechanics is rather extensive[11] the most popular of which are M-theory and loop quantum gravity. All these theories attempt to describe quantum features of gravitational interactions without necessarily aiming at the unification of all forces in nature. Among these theories string theory is the one that tries to develop a framework for the unified description of fundamental forces. Although the string theory[12] is a major attempt to incorporate gravity in a unified theory of everything, it has confronted major objections in recent years due to inconsistent predictions[13].

Decades of slow developments in the field of quantum gravity, despite extensive efforts, may be an indication of the fact that one has to choose a different path in seeking a unified theory. The research is now aligning its engine towards different effective approaches in the field within the newly emerging framework of phenomenological quantum gravity[14]. The apparent incompatibility of quantum mechanics with gravity and the failure of quantum field theories in the unification of fundamental forces with gravity may be revisited by studying underlying dissimilarities between the forces in the first place. While quantum mechanics is a theory with statistical representation of experimental results, one is to look for statistical features of gravity as a counterpart to be compared with quantum mechanics. To have a statistical view of gravity one has to think of a very large-scale universe in which galaxies play the role of particles in a gravitational fluid. Only, in that case, one can grasp the statistical effects similar to quantum mechanics. Over the past century, pioneering developments[15–31] in the field of collective quantum phenomena in environments with electromagnetic interactions has been originated. The collective quantum phenomena find numerous applications in the study of electromagnetic interactions in complex plasmas in both laboratory[32–43] and astrophysical[44–49] scales. A similar development has been motivated for the investigation of collective gravitational quantum excitations. One such approach is through the so-called nonlinear integrodifferential Schrödinger-Newton equation, analogous to the Schrödinger-Poisson[50,51] model of quantum plasmas, which has been put into attention by Diosi[52] for the first time and has been motivated by Roger Penrose[53] in connection with the wave-function collapse in gravitationally interacting quantum systems. Recently, Bahrami et. al[54] have argued against the wave-function collapse description of the Schrödinger-Newton model. Moreover, while quantum mechanics and quantum filed theories have achieved tremendous success in description of single-particle behavior at the fundamental level and the Standard Model of particle physics, respectively, their interrelating connection regarding the collective behavior of particles has been a challenging matter[55,56]. On the other hand, the spin-statistics theorem[57] probably points to our incomplete picture of underlying principles, as pointed out by Richard Feynman et al.[58]. It is however a mandate to improve current field theoretical models in order to achieve the desired accuracy before arriving at the unified picture of fundamental forces.

The study of the electrostatic quantum excitations (plasmon) within the Schrödinger-Poisson model has revealed very interesting collective quantum phenomena[59–67]. The newly developed quasiparticle model of collective excitations has been used for treating the quantum many-body effects in a completely different manner[68,69]. Although the current quasiparticle model is a many-body approach conventionally used in the condensed matter field in connection with the energy band structure concept, it has the advantage of allowing the comparison of gravity and electrostatic forces as collective interaction fields in an equal footing. There are already research showing the emergent gravitational phenomena related to the condensed matter field[70] and the quantum entanglement[71]. In the current research, we extend the quasiparticle model to collective gravitational quantum excitations called gravity quasiparticles (GQ) in a quite similar manner as in the electrostatically interacting electron gas. In doing so we can compare different aspects of collective quantum effects in gravitational and electrostatic fluids and discover possible divergence in the unification process. The quasiparticle model for gravitationally interacting fluid is presented in section "Gravitational quasiparticle model". Nonrelativistic and relativistic matter wave dispersion is deduced and compared for plasmons and GQs in sections "Nonrelativistic matter-wave dispersion" and "Relativistic matter-wave dispersion", respectively. Propagation of nonrelativistic 1D gravity excitations is studied in section "Nonrelativistic quasiparticle excitations". The phase space evolution of GQs is analyzed in section "Phase-space evolution of gravitational quasiparticles". The generalized probability current for GQs and Lemaitre-Hubble-like relation is obtained in section "Gravitational quasiparticle probability current". The GQ interference is studied in section "Gravitational quasiparticle interference" and conclusions are drawn in section "Conclusion".

Gravitational quasiparticle model

Collective excitations under the Hamiltonian action on individual particles interacting via the self-consistent potential can be modeled through the quantum multistream concept. In this model, to circumvent the many-body difficulties, instead of position representation of particles which leads to a Hartree-like product form of system wavefunction, we use multistream representation in momentum space to obtain a summed form of the total wavefunction[68]. Using the simplest form of Hamiltonian, $\mathcal{H} = \mathcal{K} + \mathcal{U}$, where $\mathcal{K}$ and $\mathcal{U}$ are respectively the kinetic and (self-consistent) potential operators, we have a single-particle Schrödinger equation

$$i\hbar \frac{\partial \mathcal{N}_j(\mathbf{r}, t)}{\partial t} = \mathcal{H}\mathcal{N}_j(\mathbf{r}, t), \tag{1}$$

where $\hbar$ is the reduced Planck constant. In the case of a gravitational interactions we have $\mathcal{U}_G = m\phi_G + \mu$, whereas for the electrostatic one, $\mathcal{U}_E = -e\phi_E + \mu$, where m is the mass, e is the electric charge and μ represents the corresponding chemical potential of the quantum gas, in their respective concepts. Moreover, Φ_G and Φ_E denote the gravitational and electrostatic interaction potentials, respectively. The nonrelativistic Hamiltonian for gravitating fluid is $\mathcal{H}_G = -(\hbar^2/2m)\Delta + m\phi_G + \mu$, whereas, for the electron gas is, $\mathcal{H}_E = -(\hbar^2/2m)\Delta - e\phi_E + \mu$

. However, the relativistic case can be treated semiclassically using the square-root Klein-Gordon Hamiltonian of $\mathcal{H}_G = \sqrt{m^2c^4 - \hbar^2c^2\Delta} + m\phi_G + \mu$ in which c denotes the speed of light in vacuum. In the quasiparticle model of collective excitations the single-particle Schrödinger equations are coupled through the Poisson's relation

$$\Delta\phi_G(\mathbf{r}) = 4\pi Gm\left[\sum_{j=1}^{N}\mathcal{N}_j(\mathbf{r},t)\mathcal{N}_j^*(\mathbf{r},t) - n_0\right], \tag{2}$$

where n_0 denotes the static equilibrium background number density. Redefining probability density of the collective mode as, $\mathcal{N}(\mathbf{r},t) = \sum_{j=1}^{N}\mathcal{N}_j(\mathbf{r},t)$ and using the standard definition, $n = \sum_{j=1}^{N}\mathcal{N}_j(\mathbf{r},t)\mathcal{N}_j^*(\mathbf{r},t)$, we arrive at the following set of coupled differential equations

$$i\hbar\frac{\partial\mathcal{N}(\mathbf{r},t)}{\partial t} = \mathcal{H}_G\mathcal{N}(\mathbf{r},t), \tag{3a}$$

$$\Delta\phi_G(\mathbf{r}) = 4\pi Gm\left[\mathcal{N}(\mathbf{r},t)\mathcal{N}^*(\mathbf{r},t) - \sum_{k\neq j}^{N}\mathcal{N}_k(\mathbf{r},t)\mathcal{N}_j^*(\mathbf{r},t) - n_0\right]. \tag{3b}$$

In the limit of large number of particles $N \gg 1$, the second term in the rhs of Poisson relation vanishes[68,69], leading to the system

$$i\hbar\frac{\partial\mathcal{N}(\mathbf{r},t)}{\partial t} = \mathcal{H}_G\mathcal{N}(\mathbf{r},t), \tag{4a}$$

$$\Delta\phi(\mathbf{r}) = 4\pi Gm\left[|\mathcal{N}(\mathbf{r},t)|^2 - n_0\right]. \tag{4b}$$

The system (4) is equally valid for nonrelativistic and relativistic Hamiltonian. Other forms of potential and quantum effect can be easily incorporated into this quasiparticle model.

The current quasiparticle model should not be confused with the wave-kinetic, Wigner-Poisson kinetic and its derivative quantum hydrodynamic theories and Madelung fluid transformation of the Schrödinger-Poisson and Schrödinger-Newton systems. These models which are categories under a same mathematical formalism lead to a generalized Bohm-Gross-type dispersion relation[72–75] suggesting the so-called quantum Jeans instability phenomenon. While the Jeans instability is originally a classical phenomena, some authors have used the quantum hydrodynamic to obtain its quantum version, although, its physical implications are not usually discussed. It is important to note that the use of Madelung's transformations to build collective quantum model from single-particle formulation is not mathematically rigorous and these transformations only become physically meaningful in connection with the quantum hydrodynamic framework[51]. The quasiparticle model, on the other hand, is a mathematically rigorous framework[68] based on a dual lengthscale theory in which the self-consistent interaction potential is fully quantized[59]. This model uses the energy band structure concept, a rigorous method in condensed matter physics, which is related to the matter wave energy dispersion. Quasiparticles in this model are field-induced particle-like entities that can interact with electrons and charged particles in the case of an electrostatic field and with matter in the case of a gravitational one. Due to both the wave-like and particle-like nature of quasiparticle excitations, caused respectively by collective and single-particle oscillations, they are characterized by two distinct de Broglie's wavelengths related through a simple complementarity-like relation[63]. The dual lengthscale quasiparticle theory has recently emerged due to apparent discrepancy in the static charge screening via the generalized Bohm-Gross-type dispersion relation, as predicted by the linearized quantum hydrodynamic formulation, which has led to intense debate among researchers of related fields over the past decade[76–83]. It has been shown that the dispersion relation of fast and slow plasmon excitations in the degenerate electron gas, consistent with the Lindhard dielectric response theory, is obtained by considering the high and low phase-speed expansions of the dielectric function. This consequently leads to an extra correction factor to the quantum Bohm term in the hydrodynamic formulation and consequently in the generalized Bohm-Gross-type dispersion relation[36]. However, this correction is usually ignored in most quantum hydrodynamic dispersion calculations[73,75]. The double-tone nature of quantum oscillations suggests a dual lengthscale quasiparticle theory for collective quantum plasmon excitations which has led to the development of the current quasiparticle model over the past few years. More recently, it has been shown that[68] the linear response theory using the quasiparticle model can go well beyond the random phase approximation (RPA) by predicting a dual-tone oscillatory Lennard-Jones-type screening of impurity charges caused by both small-scale Friedel oscillations, due to single electron excitations, modulated over the London-type attractive potential, due to collective oscillations, around the screened charge. It has also been shown that[84] the Bohm-Gross-type dispersion relation obtained via quantum kinetic and Lindhard dielectric theories is inconsistent with the experimental result of the small wavenumber plasmon dispersion of valence electrons in some simple alkali metals. The quasiparticle model has been further used to study the semi-classical relativistic quantum electron gas excitations using the square-root Klein-Gordon equation to predict a generalized equation of state for collective quantum excitations in extremely dense electron gas[69]. On the other hand, the dual lengthscale quasiparticle model has the major advantage over the Wigner-Poisson kinetic approach in which the self-

consistent potential is approximated by the Taylor series keeping only the leading order term proportional to $\hbar^2$ in the series. This semiclassical expansion of the Wigner potential in either position or momentum direction, keeping the other one fixed, is inconsistent with Heisenberg's uncertainty principle and is the main cause of the aforementioned discrepancy. It has been remarked that[85] all terms proportional to the Plank constant in the expansion of the Wigner potential are of importance regardless of the $\hbar$ order. Obtaining the classical limit of the quantum evolution equation leads to a well-known squeezing effect in quantum statistical distribution which is extensively discussed in Ref.[86]. Recently, the quasiparticle approach to the statistical evolution of electron gas using the modified Wigner distribution has been proposed for the phase-space analysis of collective quantum excitations without resorting to the Wigner potential or distribution approximation[87]. The quasiparticle model of collective quantum excitations is still in its initial development stages and may be generalized to include full electromagnetic interactions and spin-exchange effects. However, in the current analysis, we use the simplified version of the model to probe possible dissimilarities between collective quantum electrostatic and gravitational excitations. It is shown that, although collective excitations in the gravitational field via the Schrödinger-Newton formalism can be quantized similarly to that of the electrostatic field in the Schrödinger-Poisson system, either the single-particle or collective branch of gravitational quantum excitations is strongly damped (leading to either large-scale expansion or collapse). This may be one of the underlying reasons why gravity apparently defies to be unified with other fundamental forces of nature.

Nonrelativistic matter-wave dispersion

Considering the nonrelativistic quasiparticle excitations in a gravitating quantum fluid, we have the following system

$$i\hbar\frac{\partial\mathcal{N}}{\partial t} = -\frac{\hbar^2}{2m}\Delta\mathcal{N} + m\phi_G\mathcal{N} + \mu\mathcal{N}, \tag{5a}$$

$$\Delta\phi_G = 4\pi Gm\left[|\mathcal{N}|^2 - n_0\right]. \tag{5b}$$

We now linearize the system keeping the first-order terms in the perturbed variables, $\mathcal{N} = \sqrt{n_0} + \mathcal{N}_1$, $\phi_G = 0 + \phi_{G1}$, $\mu = \mu_0$, which leads to

$$i\hbar\frac{\partial\mathcal{N}_1}{\partial t} = -\frac{\hbar^2}{2m}\Delta\mathcal{N}_1 + m\phi_{G1}\sqrt{n_0} + \mu_0\mathcal{N}_1, \tag{6a}$$

$$\Delta\phi_{G1} = 4\pi Gm\sqrt{n_0}\mathcal{N}_1. \tag{6b}$$

We then Fourier analyse using the operations, $\nabla \to ik$ and $\partial/\partial t \to -i\omega$, to get

$$i\hbar\omega\mathcal{N}_1 = \frac{\hbar^2k^2}{2m}\mathcal{N}_1 + m\phi_{G1}\sqrt{n_0} + \mu_0\mathcal{N}_1, \tag{7a}$$

$$-k^2\phi_{G1} = 4\pi Gm\sqrt{n_0}\mathcal{N}_1. \tag{7b}$$

Using a scaled wavefunction $\mathcal{N}_1 \to \sqrt{n_0}\Psi$ and $\epsilon = \hbar\omega$, we get new set of equations

$$(\epsilon - \mu_0)\Psi = \frac{\hbar^2k^2}{2m}\Psi + m\phi_{G1}, \tag{8a}$$

$$-k^2\phi_{G1} = 4\pi Gmn_0\Psi. \tag{8b}$$

Final normalization of the potential as $\phi_{G1} \to E_0\Phi_G/m$ where $E_0 = \hbar\sqrt{4\pi G\rho_0}$, for GQ, with $\rho_0 = mn_0$ being the equilibrium mass density, results in

$$2E\Psi = k^2\Psi + \Phi_G, \quad -k^2\Phi_G - \Psi = 0, \tag{9}$$

where $E = (\epsilon - \mu_0)/2E_0$ and the wavenumber is scaled to the characteristic value of $k_0 = \sqrt{2mE_0}/\hbar$. Solving the system (9) gives the energy dispersion relation as $E = k^2/2 - 1/2k^2$. A quite similar dispersion for plasmon in electron gas has been found[59] in the form $E = k^2/2 + 1/2k^2$ where the energy is normalized to $2E_p$ with $E_0 = \hbar\omega_p$ ($\omega_p = \sqrt{4\pi e^2n_0/m_e}$) being the characteristic plasmon energy and the wavenumber being scaled to the plasmon wavenumber $k_0 = \sqrt{2m_eE_p}/\hbar$. One should note that for the electron gas, m_e represents the electron rest mass whereas *m* for GQ can represent particle masses, i.e., average masses of large-scale objects such as stars and galaxies depending on the scale-length of the fluid. The unified form of matter-wave dispersion is written in the form of $E = k^2/2 \mp 1/2k^2$, where minus/plus signs refer to the gravity/electrostatic quasiparticle dispersion. The first common term in the dispersion is due to the single-particle excitations whereas the second term represents the large-scale wave-like excitations[63].

The unified nonrelativistic matter-wave dispersion along with the effective mass, phase, and group speeds of quasiparticle(collective) excitations are shown in Fig. 1 for both gravitational as well as electrostatic fluids. Figure 1a shows the matter-wave dispersion plasmon (thin curve), GQ (thick curve), and parabolic free particle (dashed curve) quasiparticle excitations. The electrostatic quasiparticle dispersion has an energy gap above the Fermi level ($E = 0$)[62]. The ground state energy orbital $E = 1$ leads to the quantum beating effect. For larger

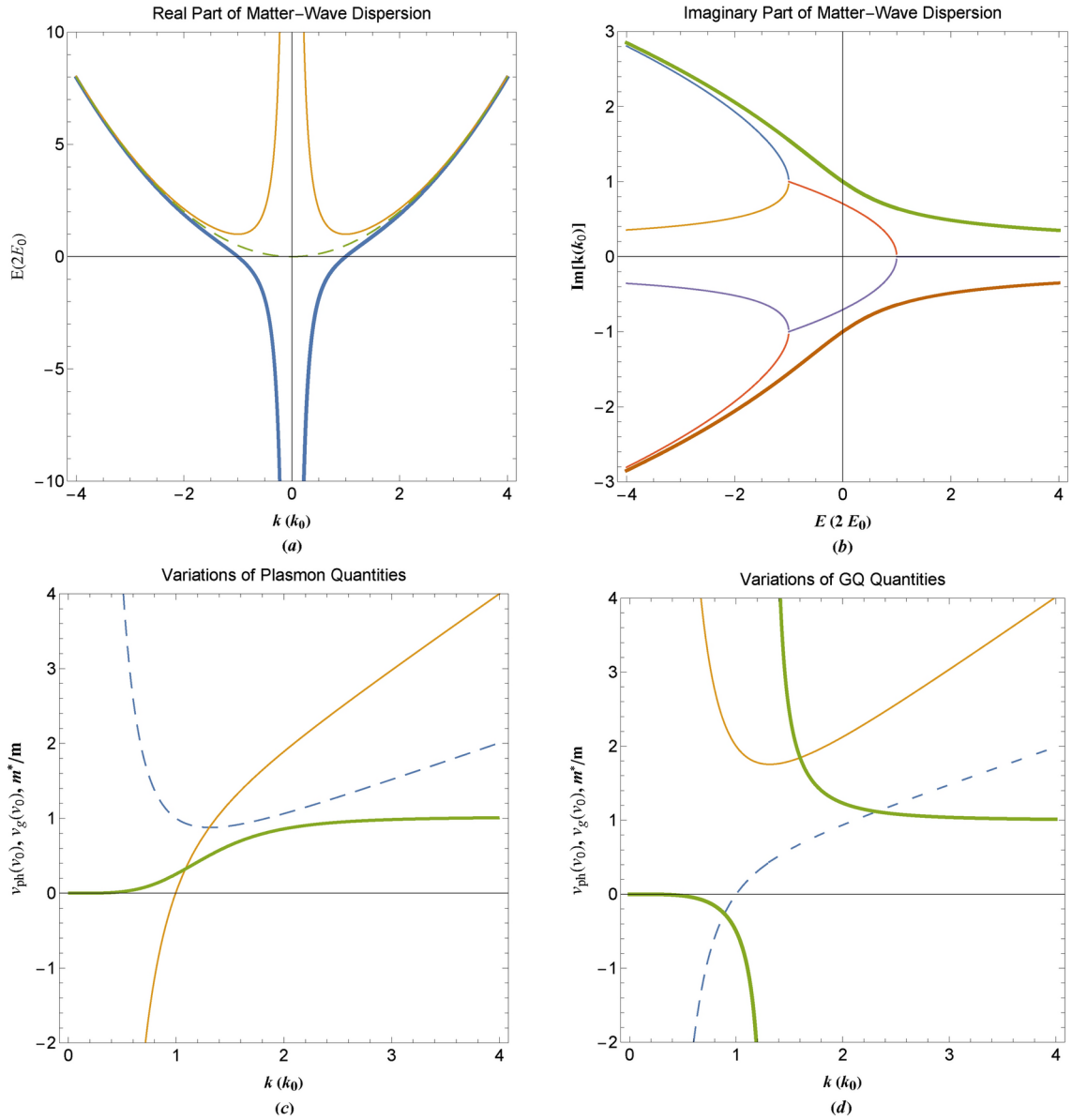

Fig. 1. (**a**) The real part of matter-wave dispersion of electrostatic (thin curves), gravitational (thick curves) and free particle (dashed curve) nonrelativistic quasiparticle excitations. (**b**) The imaginary part of matter-wave dispersion of electrostatic (thin curves) and gravitational (thick curves) nonrelativistic quasiparticle excitations. (**c**) Effective mass (thick curve), phase speed (dashed curve), and group speed (thin curve) of nonrelativistic electrostatic quasiparticles (plasmons). (**d**) Effective mass (thick curve), phase speed (dashed curve), and group speed (thin curve) of nonrelativistic gravitational quasiparticles (GQ).

energy values $E > 1$ there are distinct dual length scale particle-like and wave-like excitations corresponding respectively to the wavenumbers $k_1 = \sqrt{E - \sqrt{E^2 - 1}}$ and $k_2 = \sqrt{E + \sqrt{E^2 - 1}}$. Note that a complementarity-like relation holds between the two de-Broglie's wavelength $k_1 k_2 = 1$, in normalized form. It is noted that electrostatic excitation dispersion approaches the free electron value for large energies. As for the gravitational collective excitations, quasiparticles which are called GQs, the dispersion relation indicates the single-tone nature, unlike the electrostatic case. The characteristic wavenumbers in this case are $k_1 = \sqrt{E - \sqrt{E^2 + 1}}$ and $k_2 = \sqrt{E + \sqrt{E^2 + 1}}$ satisfying the relation $k_1 k_2 = i$. This dissimilar aspect of GQs has far-reaching consequences for gravitational interactions as will be noted later in this analysis. This fundamental feature may also be the reason that prohibits GQs from second quantization like electromagnetic interactions. It is also remarked that GQs can take zero or negative energy values. The imaginary part of dispersions corresponding to Fig. 1a are shown in Fig. 1b. The imaginary dispersion branches indicate instability of collective excitations in the system in either the form of damping or growing. It has been recently shown that in the half-space excitations, the growing instability can lead to a photo-plasmonic effect[65]. For GQs, the instability occurs for wave-like branches for positive energies $E > 0$, whereas, it takes place for particle-like branches for negative GQ energies. For the

zero energy orbital, no instability exists. Figure 1c shows the variations in effective mass (thick curve), phase speed (dashed curve), and group speed (thin curve) of collective electrostatic excitations. The speeds are given in normalized unit $v_0 = \hbar k_0/m$. The effective mass vanishes at the long wavelength limit and approaches the free particle value in the small wavelength limit. The phase speed has a minimum value at the characteristic plasmon wavenumber $k \simeq 1.316 k_p$. The group speed has negative/positive values below/above the plasmon wavenumber $k = k_p$. Figure 1d depicts the variations in effective mass (thick curve), phase speed (dashed curve), and group speed (thin curve) of collective gravity excitations. It is remarked that the effective mass of GQs is negative/positive below/above the critical wavenumber $k \simeq 1.316 k_p$. Mechanics in the universe containing negative mass have been investigated by Bonner as early as 1988[88]. The cosmological attribution of negative mass to dark energy and dark matter has also been suggested[89] and criticized[90]. The effective negative mass of electrons in plasma electron oscillations has been recently reported[91]. Figure 1d shows that the phase speed has a positive/negative value above/below the characteristic wavenumber $k = k_0$, whereas, the group speed is always positive and has a minimum value at $k \simeq 1.316 k_0$.

Relativistic matter-wave dispersion

Let us now consider relativistic quasiparticle excitations in a gravitational quantum system of particles using the square-root Klein-Gordon (SRKG) Hamiltonian. The use of the semiclassical model of SRKG instead of the Klein-Gordon and Dirac models is due to the straightforward quantization of the electrostatic field in the Hamiltonian formalism from one hand and the similar form of the resulting energy band structure to the nonrelativistic case for close comparison from the other. The wave-kinetic approach to relativistic quantum plasmas has been developed in[92]. More recently the SRKG model has been used to study the relativistic collective quantum excitations and some thermodynamic quantities in the electron gas[69]. The SRKG system for GQs is given as follows

$$i\hbar\frac{\partial \mathcal{N}}{\partial t} = \sqrt{m^2c^4 - \hbar^2c^2\Delta}\,\mathcal{N} + m\phi_G\mathcal{N} + \mu\mathcal{N}, \tag{10a}$$

$$\Delta\phi_G = 4\pi G m\left[|\mathcal{N}|^2 - n_0\right]. \tag{10b}$$

Linearizing the system by keeping the first-order terms in perturbed variables, $\mathcal{N} = \sqrt{n_0} + \mathcal{N}_1$, $\phi_G = 0 + \phi_{G1}$, $\mu = \mu_0$, leads to

$$i\hbar\frac{\partial \mathcal{N}_1}{\partial t} = \sqrt{m^2c^4 - \hbar^2c^2\Delta}\,\mathcal{N}_1 + m\phi_{G1}\sqrt{n_0} + \mu\mathcal{N}_1, \tag{11a}$$

$$\Delta\phi_{G1} = 4\pi G m\sqrt{n_0}\mathcal{N}_1. \tag{11b}$$

Using the Fourier analysis by the operations, $\nabla \to ik$ and $\partial/\partial t \to -i\omega$, we get

$$\hbar\omega\mathcal{N}_1 = mc^2\sqrt{1 + \frac{\hbar^2k^2}{m^2c^2}}\,\mathcal{N}_1 + m\phi_{G1}\sqrt{n_0} + \mu\mathcal{N}_1, \tag{12a}$$

$$-k^2\phi_{G1} = 4\pi G m\sqrt{n_0}\mathcal{N}_1. \tag{12b}$$

We then scale the wavefunction as $\mathcal{N}_1 \to \sqrt{n_0}\Psi$ and use $\epsilon = \hbar\omega$ to get new set of equations

$$(\epsilon - \mu)\Psi = mc^2\sqrt{1 + \frac{\hbar^2k^2}{m^2c^2}}\,\Psi + m\phi_{G1}\Psi, \tag{13a}$$

$$-k^2\phi_{G1} = 4\pi G\rho_0\Psi. \tag{13b}$$

Note that the factor $\sqrt{1 + v^2/c^2}$ appears as a quantum mechanical operator in the first term in rhs of (10) and implicitly in (12) and (13) through the definition $v = \hbar k/m$. This quantity which may be called the relativistic energy factor (not to be confused with the relativistic gamma factor) also appears in Ref.[72] through the wave-kinetic approach. By normalization $\phi_{1G} \to E_g\Phi_G/m$ where $E_g = m_gc^2$ (where m_g is the galactic mass, for instance) is the rest energy of the particle and the wavenumber to $k \to m_gck/\hbar$, we get

$$E\Psi = \sqrt{1 + k^2}\Psi + \Phi_G, \quad k^2\Phi_G + \Gamma\Psi = 0, \tag{14}$$

where $E = (\epsilon - \mu_0)/E_g$. Solving the system (14) gives the relativistic GQ energy dispersion relation as $E = \sqrt{1 + k^2} - \Gamma_G/k^2$ where $\Gamma_G = 2E_0/E_g$ ($E_0 = \hbar\sqrt{4\pi G\rho_0}$, for GQ). A quite similar dispersion for relativistic plasmon in electron gas has been found[69] in the form of $E = \sqrt{1 + k^2} + \Gamma_E/k^2$ where $\Gamma_E = 2E_0/E_e$ ($E_0 = E_p$, for plasmon) with $E_e = m_ec^2$ being the rest energy of electrons. The unified form of matter-wave dispersion can be written in the form of $E = \sqrt{1 + k^2} \pm \Gamma/k^2$.

The relativistic matter-wave dispersion along with the effective mass, phase, and group speeds of quasiparticle(collective) excitations are shown in Fig. 2 for both gravitational as well as electrostatic collective excisions for the simple choice of $\Gamma = 1$. The normalization units for energy here are $E_1 = \{m_gc^2, m_ec^2\}$ and for wavenumber are $k_1 = \{\hbar/m_gc, \hbar/m_ec\}$ and the corresponding speed units are $v_1 = \hbar k_1/m$. Figure 2a depicts the real part of relativistic excitations for gravity (thick curve), electrostatic (thin curve), and free particle (dashed

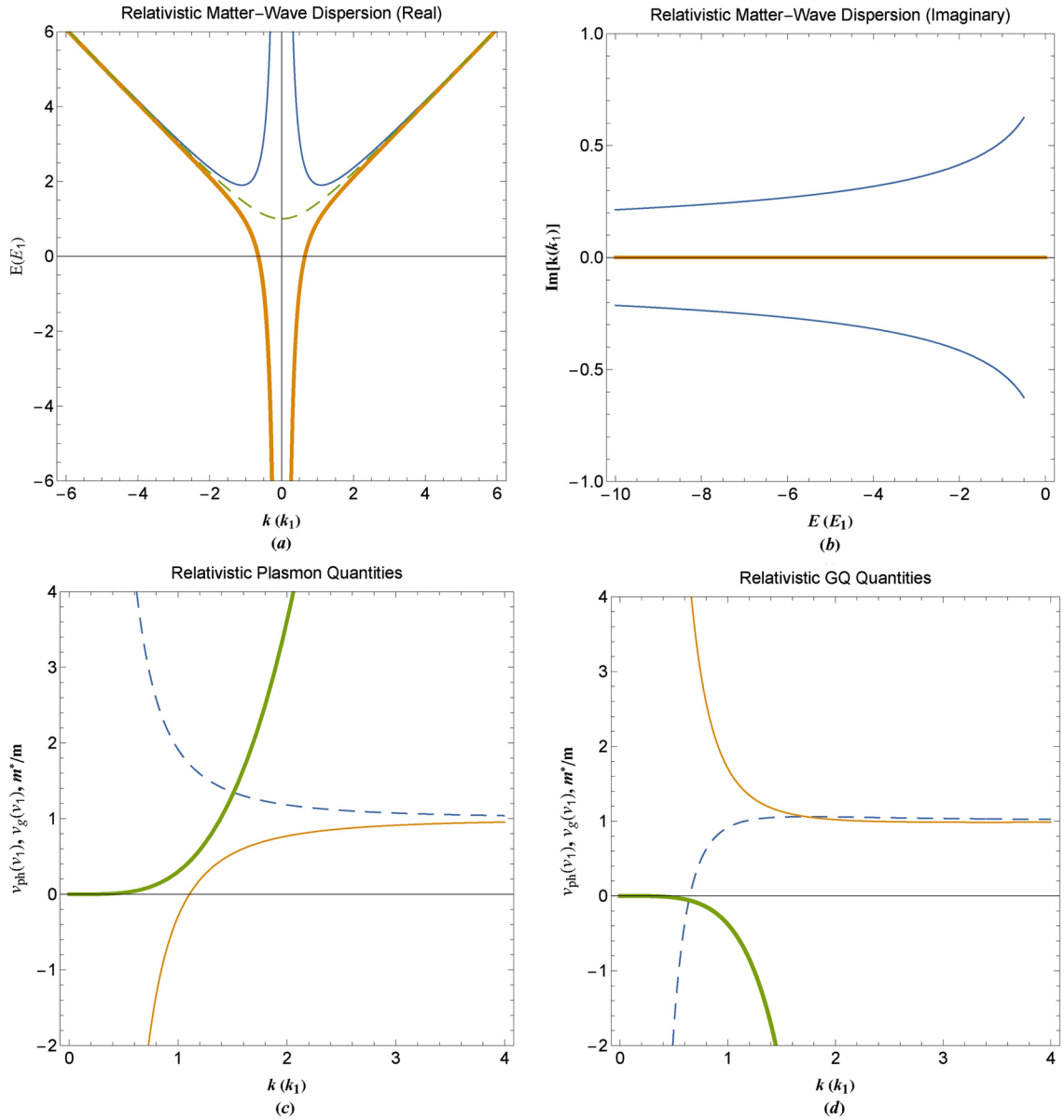

Fig. 2. (**a**) The real part of matter-wave dispersion of electrostatic (thin curves), gravitational (thick curves) and free particle (dashed curve) relativistic quasiparticle excitations. (**b**) The imaginary part of matter-wave dispersion of electrostatic (thin curves) and gravitational (thick curves) relativistic quasiparticle excitations. (**c**) Effective mass (thick curve), phase speed (dashed curve), and group speed (thin curve) of relativistic electrostatic quasiparticles (plasmons). (**d**) Effective mass (thick curve), phase speed (dashed curve), and group speed (thin curve) of relativistic gravitational quasiparticles (GQ).

curve). The only difference between Fig. 2a with 1a is that for the relativistic dispersions, the higher energy limit approaches the photon lines. Figure 2b shows the imaginary parts of the relativistic dispersion relations. It is remarked that for electrostatic excitations the imaginary wavenumbers reside in negative energy values which are ruled out in the electron gas with positive energy values. Moreover, the relativistic GQs are found to be stable for all energy orbital. Figure 2c shows the effective mass (thick curve), the phase speed (dashed curve), and the group speed (thin curve) for relativistic plasmons. The effective mass vanishes at the long wavelength limit but increases unboundedly in the small wavelength limit. The phase is always positive approaching the light speed in vacuum for $k \to \infty$. The group speed is negative/positive below/above $k = k_0$ approaching the speed of light as $k \to \infty$. Figure 2d shows the effective mass (thick curve), the phase speed (dashed curve), and the group speed (thin curve) for relativistic GQs. It is interesting to find that relativistic GQs have negative effective mass. Furthermore, the group speed of relativistic GQs is positive and higher than the speed of light in vacuum but approaching the light speed as $k \to \infty$. The phase speed, on the other hand, can be either positive or negative approaching the light speed as $k \to \infty$.

Nonrelativistic quasiparticle excitations

The nonrelativistic normalized linear Schrödinger-Poisson system admits a simple set of solutions. For instance, consider the following 1D pseudoforce system

$$i\hbar\frac{d\varphi(t)}{dt} = \epsilon\varphi(t), \tag{15a}$$

$$\frac{d^2\Psi(x)}{dx^2} \mp \Phi(x) + 2E\Psi(x) = 0, \tag{15b}$$

$$\frac{d^2\Phi(x)}{dx^2} - \Psi(x) = 0, \tag{15c}$$

where the wavefunction is assumed to be separable in the form $\mathcal{N}(x,t) = \Psi(x)\varphi(t)$ and minus/plus signs refer to gravitational/electrostatic excitations with their corresponding normalization units. The quasiparticle solution then reads

$$\begin{bmatrix} \Phi(x) \\ \Psi(x) \end{bmatrix} = \frac{1}{2\alpha}\begin{bmatrix} \Psi_0 \mp k_2^2\Phi_0 & -\left(\Psi_0 \mp k_1^2\Phi_0\right) \\ -\left(\Phi_0 + k_1^2\Psi_0\right) & \Phi_0 + k_2^2\Psi_0 \end{bmatrix}\begin{bmatrix} \exp(ik_1x) \\ \exp(ik_2x) \end{bmatrix}, \tag{16}$$

in which the minus/plus sign in the wavefunction corresponds to the GQ/plasmon case with Φ_0 and Ψ_0 are the initial values assuming, $\Phi'(0) = \Psi'(0) = 0$, for simplicity. The de Broglie's wavenumbers read

$$k_1 = \sqrt{E-\alpha}, \quad k_2 = \sqrt{E+\alpha}, \quad \alpha = \sqrt{E^2 \mp i^2}, \tag{17}$$

where again minus/plus signs refer to gravitational/electrostatic excitations. Note that the complementarity-like relation between the de Broglie's matter wavenumbers is $k_1k_2 = \sqrt{\mp 1}$.

Figure 3 shows the space variation of the solutions assuming initial conditions $\Phi_0 = \Psi_0 = 1$. Figure 3a depicts the density variations for electrostatic mode in orbital $E = 5$. The corresponding variation in electrostatic energy is shown in Fig. 3b which indicates the dual-tone nature of electrostatic potential variations. As it is remarked the fine/large structure shown in Fig. 3b corresponds to the particle-like/wave-like nature. Figure 3c, d show the corresponding variations for gravitational excitations at the same energy orbital. The monotonic variation is apparent from these plots in addition to the damping effect for the gravitational field at larger distances in Fig. 3d.Figure 4 shows the wavefunction variations at different orbital. Plot 4a shows the electrostatic mode at energy orbital $E = 2$ (for comparison) revealing the dual-tone nature of space variations. The gravitational mode at the same orbital is shown in Fig. 4b lacking the large-scale variations (as compared to Fig. 4a). This is due to an unstable wave-like branch of collective gravitational excitations for positive energy values as shown from the dispersion in Fig. 1a. This feature marks a primary difference between plasmon and GQ leading to remarkable dissimilarities between these two fundamental types of excitations. It is seen that for gravity the long-range interactions become ineffective due to this feature. Figure 4c depicts the wavefunction for $E = 0$ in which $k_1 = i$ and $k_2 = 1$. This state may be considered as the ground state in which particle-like and wave-like oscillations are complex conjugate of each other. However, at this energy orbital, the damping effect vanishes and this orbital is completely stable. Figure 4d shows the GQ wavefunction at negative energy orbital. For negative energy values the particle-like/wave-like excitations become stable/unstable quite contrary to the case of positive energy excitations. The amplitude of single-tone oscillations in this orbital is greatly reduced showing sharp damping of particle-like oscillations with the (wave-like) excitation wavelength increased. In the negative energy orbital collective gravitational excitations possess only a wave-like nature and as is depicted in Fig. 1d the GQ has a negative effective mass.Figure 5 shows the potential energy of excitations corresponding to values used in Fig. 4. For electrostatic excitations shown in Fig. 5a the variations are clearly of dual length-scale nature. However, for corresponding gravitational potential energy at the same positive energy orbital, the wave-like oscillations are transient, and only particle-like oscillations persist at long ranges. The zero-energy orbital shown in Fig. 5c is a long-wavelength excitation with monotone stability. The negative orbital GQ potential energy variations are shown in Fig. 5d which shows only wave-like oscillations.

Phase-space evolution of gravitational quasiparticles

The real-valued stationary solution of 1D gravitational collective quantum excitations for $x > 0$ is given as

$$\begin{bmatrix} \Phi(x) \\ \Psi(x) \end{bmatrix} = \frac{1}{2\alpha}\begin{bmatrix} \Psi_0 - k_2^2\Phi_0 & -\left(\Psi_0 - k_1^2\Phi_0\right) \\ -\left(\Phi_0 + k_1^2\Psi_0\right) & \Phi_0 + k_2^2\Psi_0 \end{bmatrix}\begin{bmatrix} \exp(ik_1x) \\ \cos(k_2x) \end{bmatrix}. \tag{18}$$

Here we are interested in time evolution in phase space[86] for GQ starting from the initial stationary states given in (18). To this end, we start with the normalized time-dependent system of equations,

$$2i\frac{\partial\mathcal{N}}{\partial t} = -\frac{\partial^2\mathcal{N}}{\partial x^2} + \Phi + \mu_0\mathcal{N}, \tag{19a}$$

$$\frac{\partial^2\Phi}{\partial x^2} - \mathcal{N} = 0, \tag{19b}$$

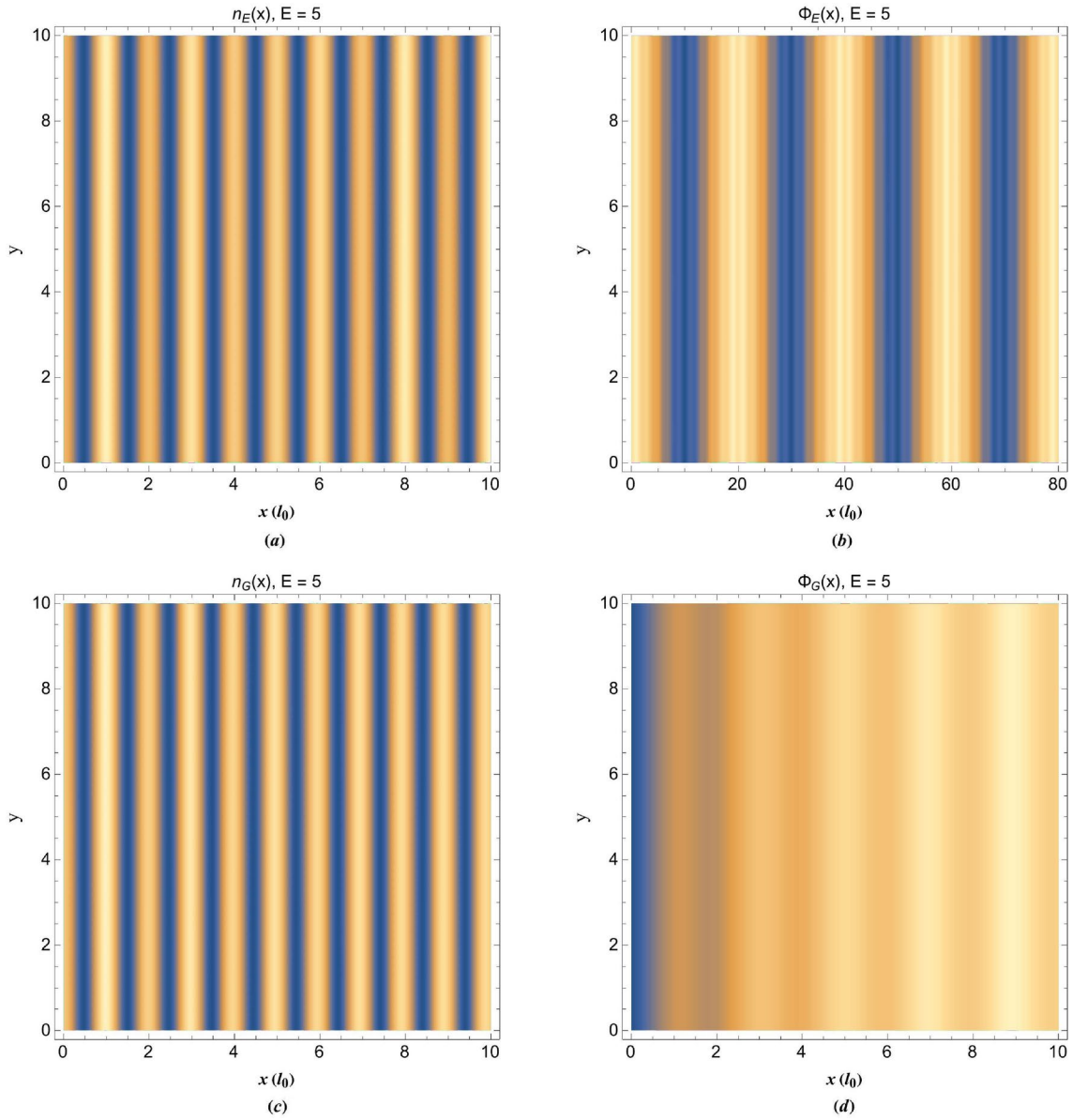

Fig. 3. (**a**) Density profile of 1D plasmon excitation at energy orbital $E = 5$. (**b**) Potential profile of 1D plasmon excitation at energy orbital $E = 5$. (**c**) Density profile of 1D GQ excitation at energy orbital $E = 5$. (**d**) Potential profile of 1D GQ excitation at energy orbital $E = 5$.

where the factor 2 appears in (19) because the time is normalized to $1/(2\omega_p)$ and Φ represents the gravitational potential. On the other hand, by the standard definition of Wigner function[93] we have in normalized form

$$W(x,v) = \int_{-\infty}^{+\infty} e^{-ivs} \mathcal{N}\left(x + \frac{s}{2}\right) \mathcal{N}^*\left(x - \frac{s}{2}\right) ds, \tag{20}$$

Using the linearized time-dependent Schrödinger equation, we have

$$2\frac{\partial \mathcal{N}_0}{\partial t} = i\frac{\partial^2 \mathcal{N}_0}{\partial x^2} - i\Phi_0 - i\mu_0 \mathcal{N}_0, \tag{21}$$

where $\mathcal{N}_0 = \mathcal{N}(x,t)$ and $\Phi_0 = \Phi(x)$. The time evolution of the Wigner function is then given by

$$\frac{\partial W}{\partial t} = \int_{-\infty}^{+\infty} e^{-ivs} \left(\mathcal{N}_+ \frac{\partial \mathcal{N}_-^*}{\partial t} + \mathcal{N}_-^* \frac{\partial \mathcal{N}_+}{\partial t}\right) ds, \tag{22}$$

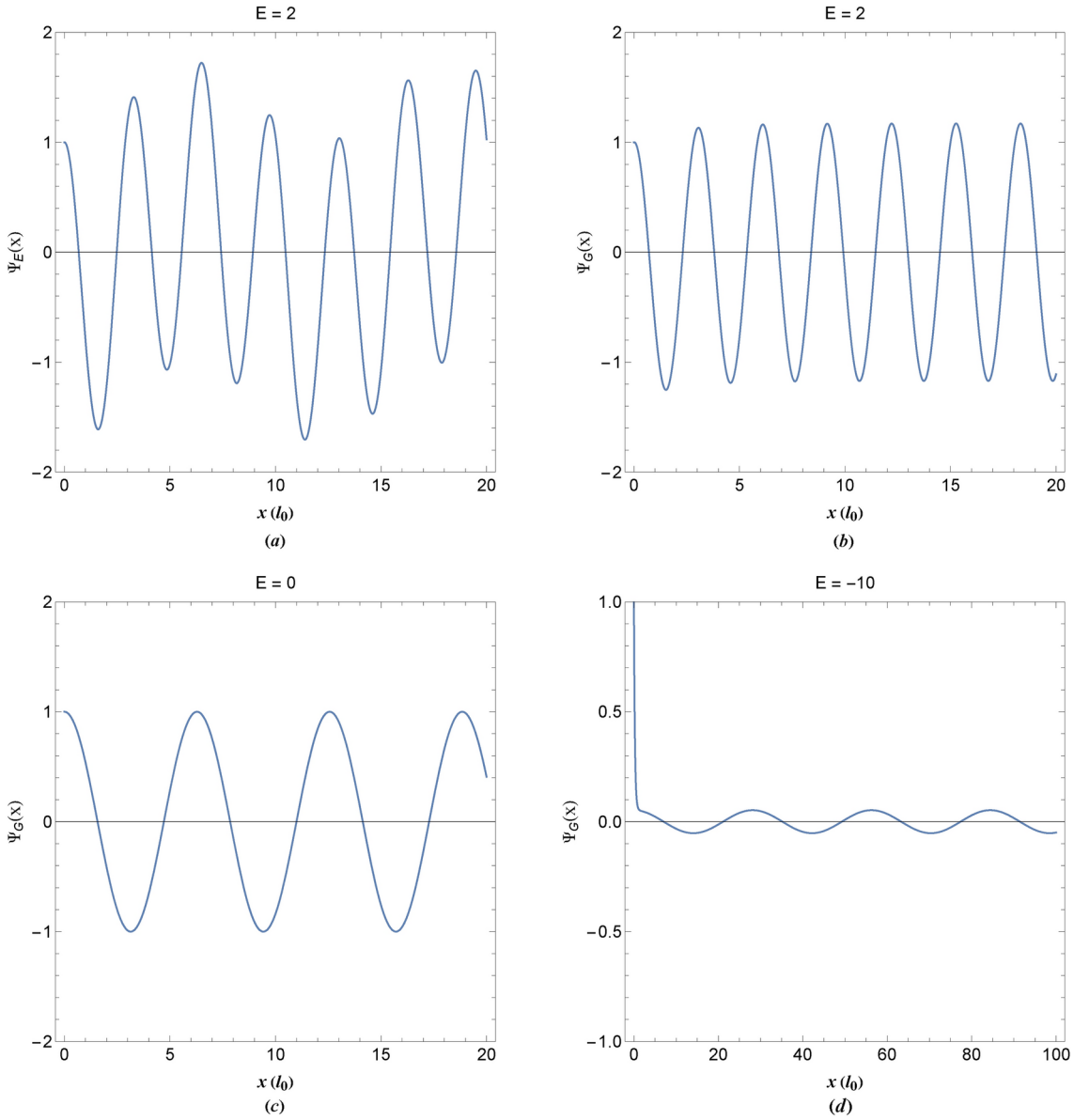

Fig. 4. (**a**) Density profile of 1D plasmon excitation at energy orbital $E = 2$. (**b**) Density profile of 1D GQ excitation at energy orbital $E = 2$. (**c**) Density profile of 1D GQ excitation at energy orbital $E = 0$. (**d**) Density profile of 1D GQ excitation at energy orbital $E = -10$.

where $\mathcal{N}_\pm = \mathcal{N}(x \pm s/2, t)$. It is readily found that

$$2\frac{\partial \mathcal{N}_-^*}{\partial t} = -i\frac{\partial^2 \mathcal{N}_-^*}{\partial x^2} + i\Phi_-^* + i\mu_0 \mathcal{N}_-^*, \tag{23a}$$

$$2\frac{\partial \mathcal{N}_+}{\partial t} = i\frac{\partial^2 \mathcal{N}_+}{\partial x^2} - i\Phi_+ - i\mu_0 \mathcal{N}_+, \tag{23b}$$

where $\Phi_\pm = \Phi(x \pm s/2)$. Consequently, we have

$$2\mathcal{N}_+\frac{\partial \mathcal{N}_-^*}{\partial t} + 2\mathcal{N}_-^*\frac{\partial \mathcal{N}_+}{\partial t} = \tag{24a}$$

$$-i\left(\mathcal{N}_+\frac{\partial^2 \mathcal{N}_-^*}{\partial x^2} - \mathcal{N}_-^*\frac{\partial^2 \mathcal{N}_+}{\partial x^2}\right) + i\left(\mathcal{N}_+\Phi_-^* - \Phi_+\mathcal{N}_-^*\right), \tag{24b}$$

Finally, we arrived at

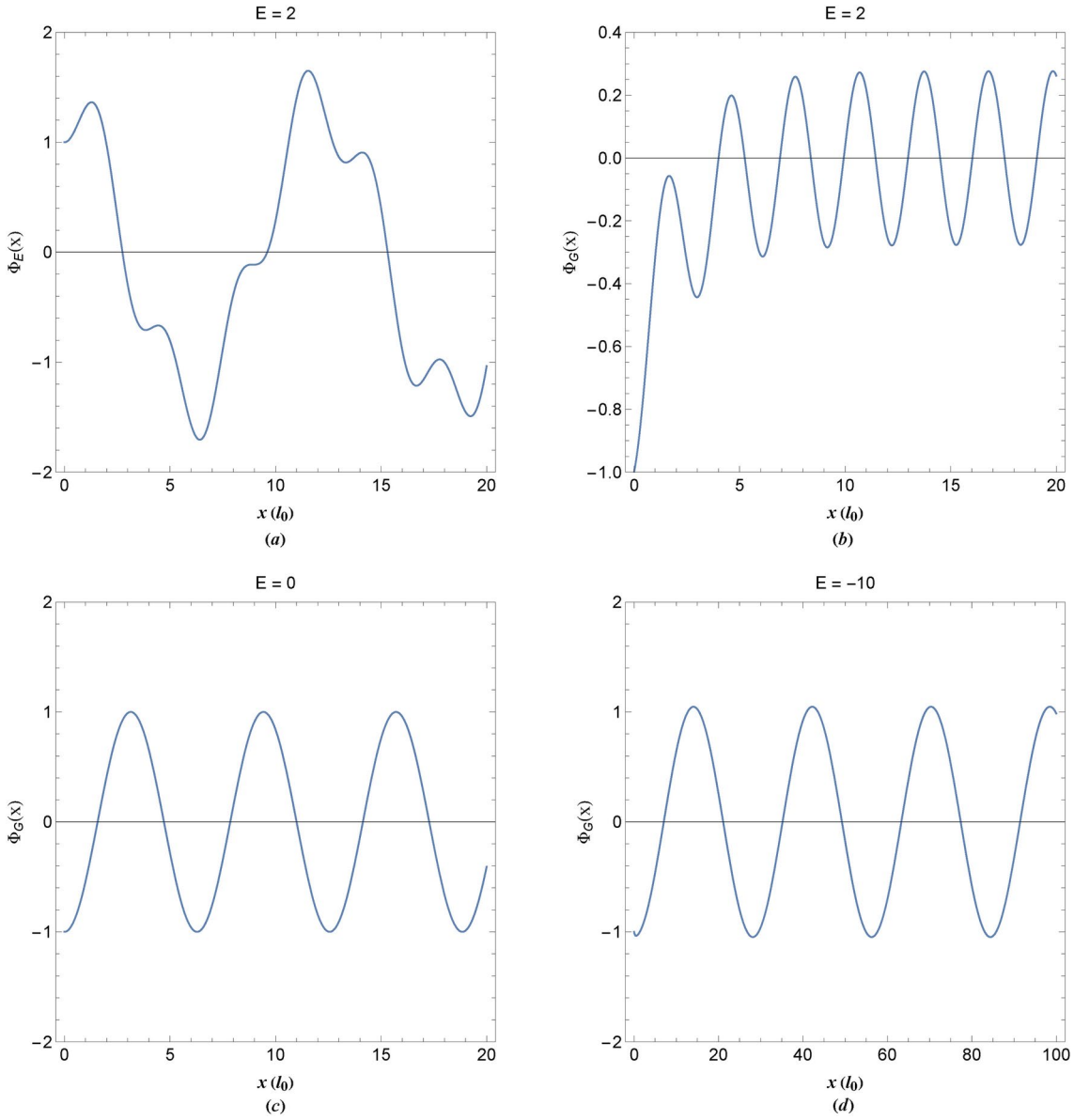

Fig. 5. (**a**) Potential energy profile of 1D plasmon excitation at energy orbital $E = 2$. (**b**) Potential energy profile of 1D GQ excitation at energy orbital $E = 2$. (**c**) Potential energy profile of 1D GQ excitation at energy orbital $E = 0$. (**d**) Potential energy profile of 1D GQ excitation at energy orbital $E = -10$.

$$2\frac{\partial W}{\partial t} = -i\int_{-\infty}^{+\infty} e^{-ivs}\left(\mathcal{N}_+\frac{\partial^2\mathcal{N}_-^*}{\partial x^2} - \mathcal{N}_-^*\frac{\partial^2\mathcal{N}_+}{\partial x^2}\right)ds + i\int_{-\infty}^{+\infty} e^{-ivs}\left(\mathcal{N}_+\Phi_-^* - \Phi_+\mathcal{N}_-^*\right)ds. \tag{25a}$$

Now using the integrations by parts, one obtains

$$\int_{-\infty}^{+\infty} e^{-ivs}\mathcal{N}_+\frac{\partial^2\mathcal{N}_-^*}{\partial x^2}ds = -2iv\int_{-\infty}^{+\infty} e^{-ivs}\mathcal{N}_+\frac{\partial\mathcal{N}_-^*}{\partial x}ds + \int_{-\infty}^{+\infty} e^{-ivs}\frac{\partial\mathcal{N}_+}{\partial x}\frac{\partial\mathcal{N}_-^*}{\partial x}ds, \tag{26a}$$

$$\int_{-\infty}^{+\infty} e^{-ivs}\mathcal{N}_-^*\frac{\partial^2\mathcal{N}_+}{\partial x^2}ds = 2iv\int_{-\infty}^{+\infty} e^{-ivs}\mathcal{N}_-^*\frac{\partial\mathcal{N}_+}{\partial x}ds + \int_{-\infty}^{+\infty} e^{-ivs}\frac{\partial\mathcal{N}_-^*}{\partial x}\frac{\partial\mathcal{N}_+}{\partial x}ds, \tag{26b}$$

which leads to

$$2\frac{\partial W}{\partial t}+2v\frac{\partial W}{\partial x}=i\int_{-\infty}^{+\infty}e^{-ivs}\left(\mathcal{N}_{+}\Phi_{-}^{*}-\Phi_{+}\mathcal{N}_{-}^{*}\right)ds. \tag{27}$$

The Poisson's equation is now used to calculate the first term in the RHS of (27)

$$\frac{\partial^2\Phi_{+}}{\partial x^2}=\mathcal{N}_{+},\quad \frac{\partial^2\Phi_{-}^{*}}{\partial x^2}=\mathcal{N}_{-}^{*}, \tag{28}$$

We then have

$$\mathcal{N}_{+}\Phi_{-}^{*}-\Phi_{+}\mathcal{N}_{-}^{*}=\Phi_{-}^{*}\frac{\partial^2\Phi_{+}}{\partial x^2}-\Phi_{+}\frac{\partial^2\Phi_{-}^{*}}{\partial x^2}. \tag{29}$$

Using (29) in (27), we arrive at

$$2\frac{\partial W}{\partial t}+2v\frac{\partial W}{\partial x}=i\int_{-\infty}^{+\infty}e^{-ivs}\left(\Phi_{-}^{*}\frac{\partial^2\Phi_{+}}{\partial x^2}-\Phi_{+}\frac{\partial^2\Phi_{-}^{*}}{\partial x^2}\right)ds. \tag{30}$$

The first term in the RHS of (30) can be treated similar to (26)

$$\int_{-\infty}^{+\infty}e^{-ivs}\Phi_{+}\frac{\partial^2\Phi_{-}^{*}}{\partial x^2}ds=-2iv\int_{-\infty}^{+\infty}e^{-ivs}\Phi_{+}\frac{\partial\Phi_{-}^{*}}{\partial x}ds+\int_{-\infty}^{+\infty}e^{-ivs}\frac{\partial\Phi_{+}}{\partial x}\frac{\partial\Phi_{-}^{*}}{\partial x}ds, \tag{31a}$$

$$\int_{-\infty}^{+\infty}e^{-ivs}\Phi_{-}^{*}\frac{\partial^2\Phi_{+}}{\partial x^2}ds=2iv\int_{-\infty}^{+\infty}e^{-ivs}\Phi_{-}^{*}\frac{\partial\Phi_{+}}{\partial x}ds+\int_{-\infty}^{+\infty}e^{-ivs}\frac{\partial\Phi_{-}^{*}}{\partial x}\frac{\partial\Phi_{+}}{\partial x}ds, \tag{31b}$$

giving the following result

$$\frac{\partial W(x,v,t)}{\partial t}+v\frac{\partial W(x,v,t)}{\partial x}+v\frac{\partial Z(x,v)}{\partial x}=0. \tag{32}$$

with a new definition

$$Z(x,v)=\int_{-\infty}^{+\infty}e^{-ivs}\Phi\left(x+\frac{s}{2}\right)\Phi^{*}\left(x-\frac{s}{2}\right)ds. \tag{33}$$

which leads to the generalized time evolution of collective quantum gravitational excitations in the form

$$\frac{\partial W(x,v,t)}{\partial t}+v\frac{\partial\left[W(x,v,t)+Z(x,v)\right]}{\partial x}=0. \tag{34}$$

By definition of a modified Wigner function, $M(x,v,t)=W(x,v,t)+Z(x,v)$, one may write

$$\frac{\partial M(x,v,t)}{\partial t}+v\frac{\partial M(x,v,t)}{\partial x}=0. \tag{35}$$

Equation (35) describes the evolution of free GQ and indeed is similar to the case of a free classical system of particles in the absence of external forces. It is concluded that the gravitation forces acting between particles do not affect the linear evolution of collective excitations. However, there should be a nonlinear effect which may be explored using the nonlinear system. The solution to the evolution equation is given as $M(x,v,t)=M(x-vt,v,0)$, where

$$M_G=\int_{-\infty}^{+\infty}e^{-ivs}\left[\Psi\left(x-vt+\frac{s}{2}\right)\Psi\left(x-vt-\frac{s}{2}\right)+\Phi\left(x-vt+\frac{s}{2}\right)\Phi\left(x-vt-\frac{s}{2}\right)\right]ds. \tag{36}$$

The corresponding modified Wigner function for plasmon is given as[87]

$$M_E=\int_{-\infty}^{+\infty}e^{-ivs}\left[\Psi\left(x-vt+\frac{s}{2}\right)\Psi\left(x-vt-\frac{s}{2}\right)-\Phi\left(x-vt+\frac{s}{2}\right)\Phi\left(x-vt-\frac{s}{2}\right)\right]ds. \tag{37}$$

Figure 6 shows the modified Wigner function for electrostatic and gravitational excitations. Figure 6a shows the distribution profile of plasmon in momentum space for $E=2$ at initial time. The momentum has

four distinct peaks at the intersection of energy level with the nonrelativistic plasmon dispersion curve shown in Fig. 1a. Figure 6b shows the probability density distribution corresponding to values in Fig. 6a showing the characteristic dual-tone feature of plasmon. Figure 6c depicts the velocity distribution of gravitational excitations at the same orbital as in Fig. 6a. Other than velocity peaks in the intersections of energy level with the GQ dispersion in Fig. 1a, there is a strong peak at the center which indicates the localization of the majority of particles in collective gravity excitations due to ineffective wave-like momentum transfer in gravitational fluids. Figure 6d indicates the decay of probability distribution due to wave-like excitation damping of gravity excitations for positive energy values.Figure 7 shows the modified distribution profile for parameter values used in Fig. 6 at a later time $t = 1$. It is remarked that at small later times the $v = 0$ probability distribution of Fig. 7b, d are not changed, significantly. It is however noted that the time evolution of GQ velocity distribution has a significant effect on spreading the particle velocity to higher positive values. This is caused by the quantum uncertainty effect where the space decay of collective mode acts as the confinement of particles around near $x = 0$ spreading the momentum to higher values in exchange. This feature is quite similar to the tunneling of electrons at the half-space metal surface where the wavefunction shows the decaying effect.Figure 8 shows the modified distribution at time $t = 0$ for different values of quasiparticle energy. The electrostatic excitations distribution profile at orbital $E = 2$ is shown in Fig. 8a indicating dominant velocity strips as white lines. There

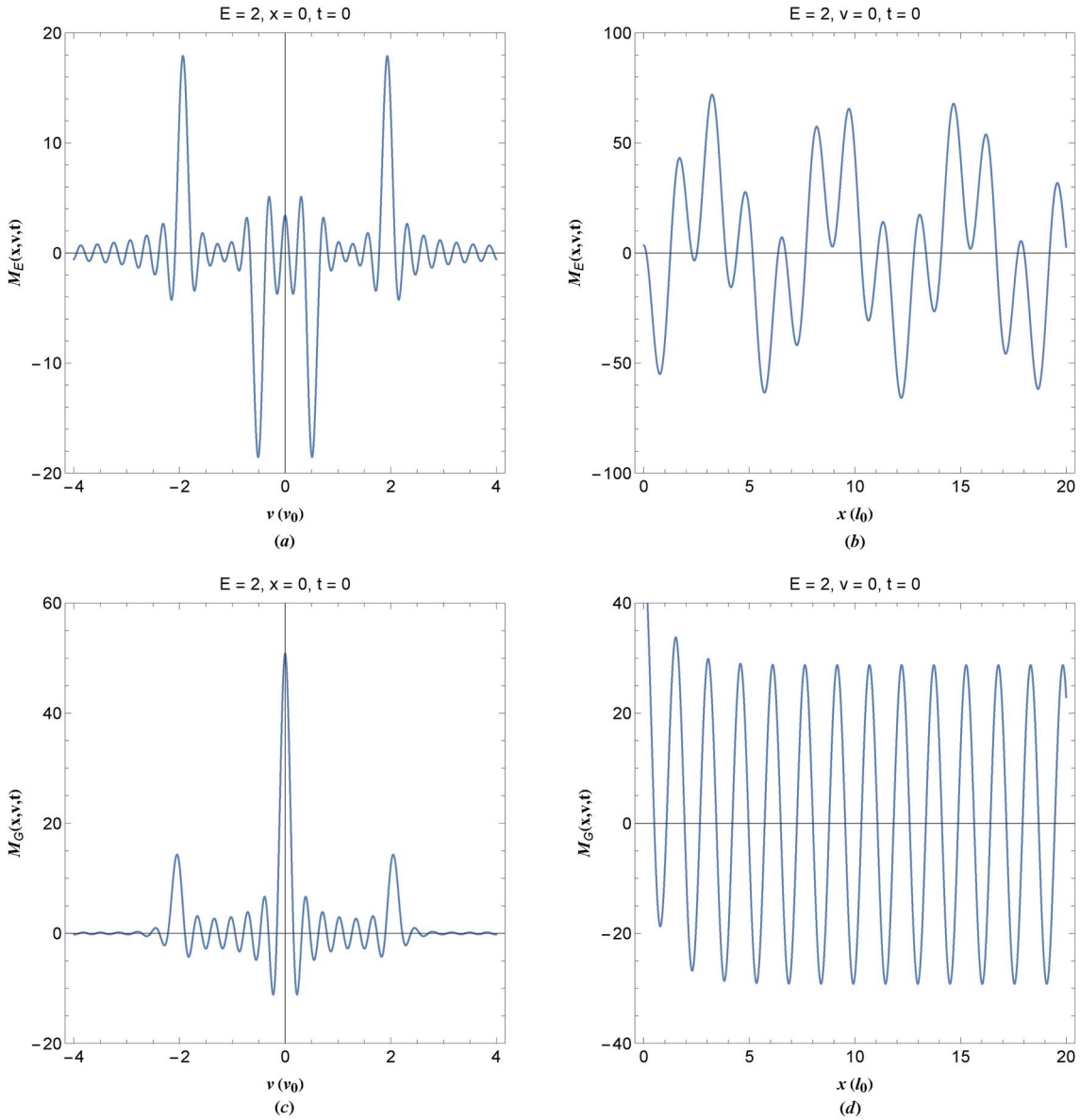

Fig. 6. (**a**) The modified Wigner function profile in momentum space for plasmon excitation at orbital $E = 2$ at time $t = 0$. (**b**) The modified Wigner function profile in position space for plasmon excitation at orbital $E = 2$ at time $t = 0$. (**c**) The modified Wigner function profile in momentum space for GQ excitation at orbital $E = 2$ at time $t = 0$. (**d**) The modified Wigner function profile in position space for GQ excitation at orbital $E = 2$ at time $t = 0$.

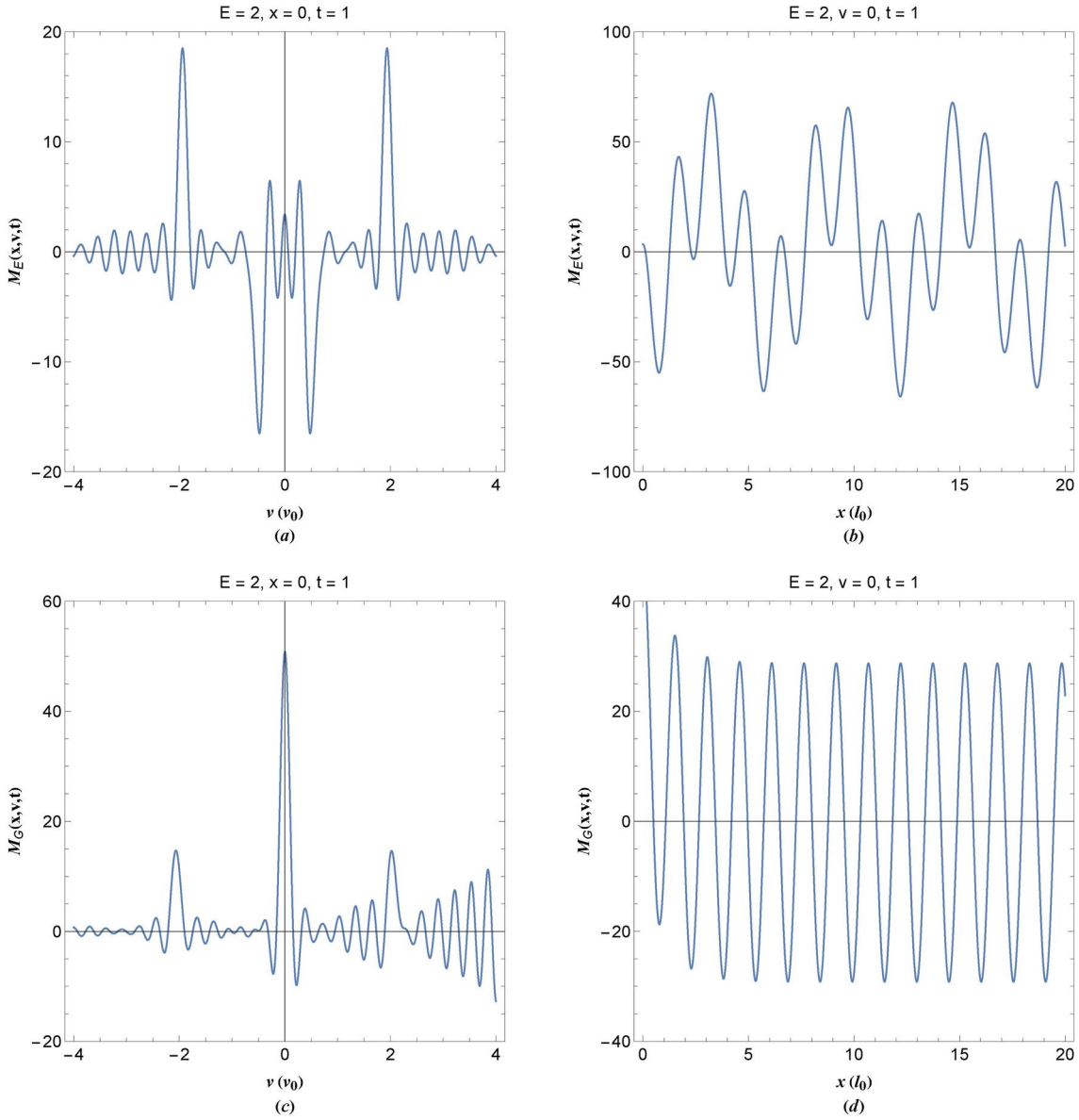

Fig. 7. (**a**) The modified Wigner function profile in momentum space for plasmon excitation at orbital $E = 2$ at time $t = 1$. (**b**) The modified Wigner function profile in position space for plasmon excitation at orbital $E = 2$ at time $t = 1$. (**c**) The modified Wigner function profile in momentum space for GQ excitation at orbital $E = 2$ at time $t = 1$. (**d**) The modified Wigner function profile in position space for GQ excitation at orbital $E = 2$ at time $t = 1$.

are strong variations between the inner velocity strips which is called the violent region. The bubble structures show the distribution peaks caused by collective excitations. The smaller/bigger bubbles are due to particle-like/wave-like oscillations in quasiparticles. Figure 8b shows the GQ distribution profile at orbital $E = 2$. Particle-like small bubbles are packed around the zero-velocity region. Figure 8c shows the modified function profile at GQ orbital $E = 0$. Two distinct velocity strips confine the violent region in which bubbles are neither wave-like nor particle-like. The modified Wigner function profile for negative energy GQ is shown in Fig. 8d. There are very large bubble structures caused by the wave-like excitations. This is because for negative energy values the particle-like excitations are strongly damped.Figure 9 shows the evolved distribution function profiles corresponding to values used in Fig. 8 at time $t = 20$. Figure 9a shows that time evolution has a grinding effect on bubbles in the violent region which is reminiscent of the Landau damping effect in the electrostatic system. A similar feature is found for GQ at the same energy orbital. However, it is remarked that the momentum spread in Fig. 9a leads to a new kind of gravitational quantum instability. Such an effect has also been recently seen to occur for half-space surface spill-out electron excitations[87] as a manifestation of the Heisenberg uncertainty principle and is interpreted as the quantum tunneling effect. The latter effect has also been attributed to the theoretically predicted[66] hot electron generation at the surface of metals and semiconductors. The presence of a similar effect for GQs may indicate large-scale expansion of matter under the influence of damped collective

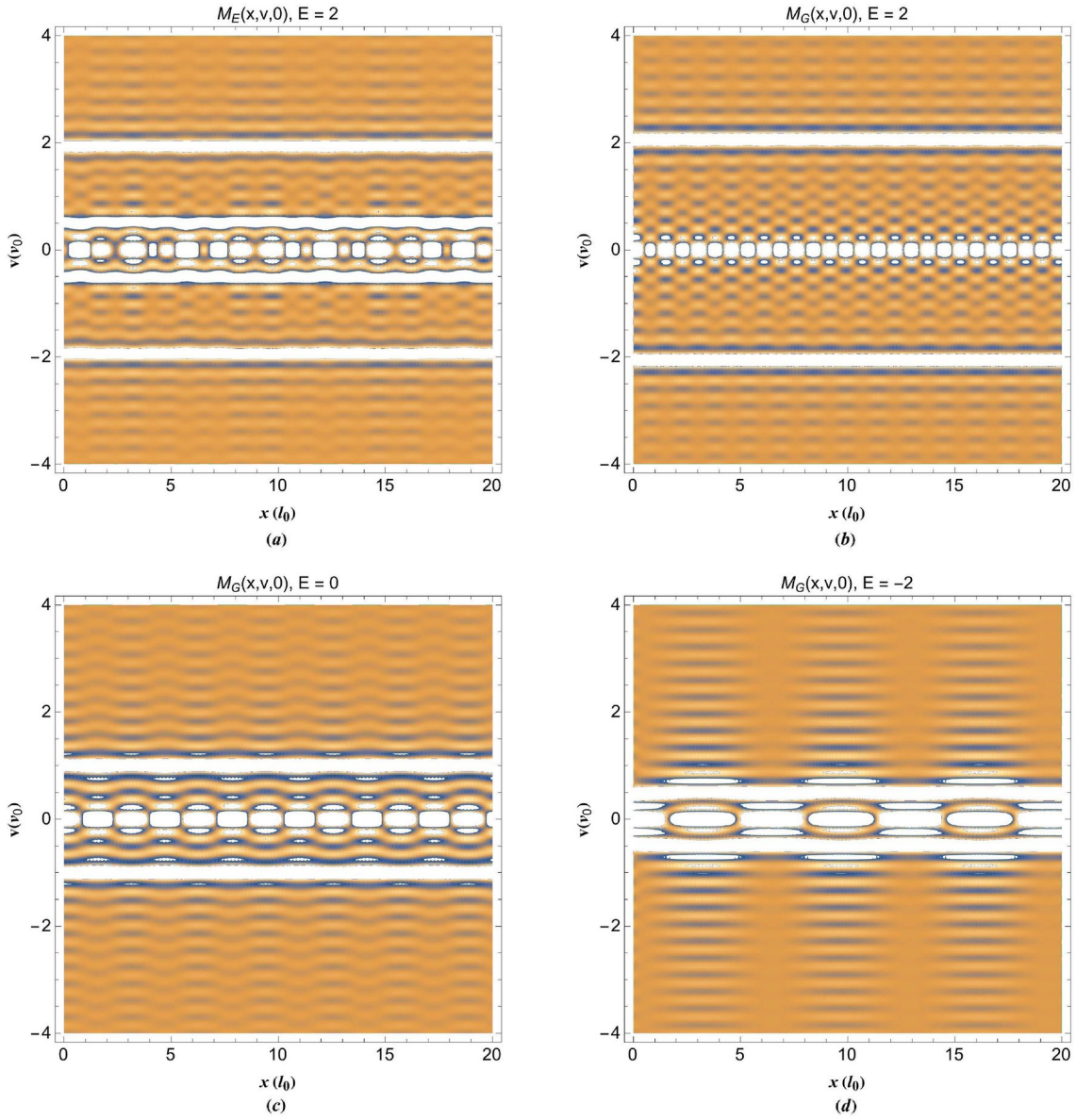

Fig. 8. (**a**) The modified Wigner function phase-space profile for plasmon excitation at orbital $E = 2$ at time $t = 0$. (**b**) The modified Wigner function phase-space profile for GQ excitation at orbital $E = 2$ at time $t = 0$. (**c**) The modified Wigner function phase-space profile for GQ excitation at orbital $E = 0$ at time $t = 0$. (**d**) The modified Wigner function phase-space profile for GQ excitation at orbital $E = -2$ at time $t = 0$.

gravity branch for positive energy dispersion band (and not the predicted Jeans collapse as suggested by previous quantum kinetic and hydrodynamic and wave-kinetic models[72–75]). This is a very interesting prediction of the gravitational quasiparticle model which is consistent with the well-known experimental observations of universal expansion[7]. This effect is caused by the divergent feature of collective damping of gravity quasiparticle excitations as compared to the electrostatic counterpart. This momentum spread due to the ineffectiveness of wave-like excitations should lead to the expansion of the gravitational fluid at positive GQ energy values. Figure 9c shows the time evolution of zero energy GQ excitation. Note that, while the grinding of a large bubble structure is also present in this case, the momentum spread is absent. This is because neither wave-like nor particle-like damping is present in collective mode at $E = 0$ (e.g. see Fig. 4c). Figure 9d reveals that momentum spread is also present for negative energy GQ orbital. It can be seen that for $E > 0$ only the particle-like branch is stable and the instability of the collective branch leads to the expansion of matter. For $E = 0$ the system is completely stable and neither expands nor collapses, whereas, for $E < 0$ the instability arises for the particle-like branch and the collective branch becomes stable therefore the negative energy band may indicate the gravitational collapse effect in the current model. In the relativistic case, the critical wavenumber for $E = 0$ where wavelike de Broglie's wavelength coincides with that of particle-like, is given by

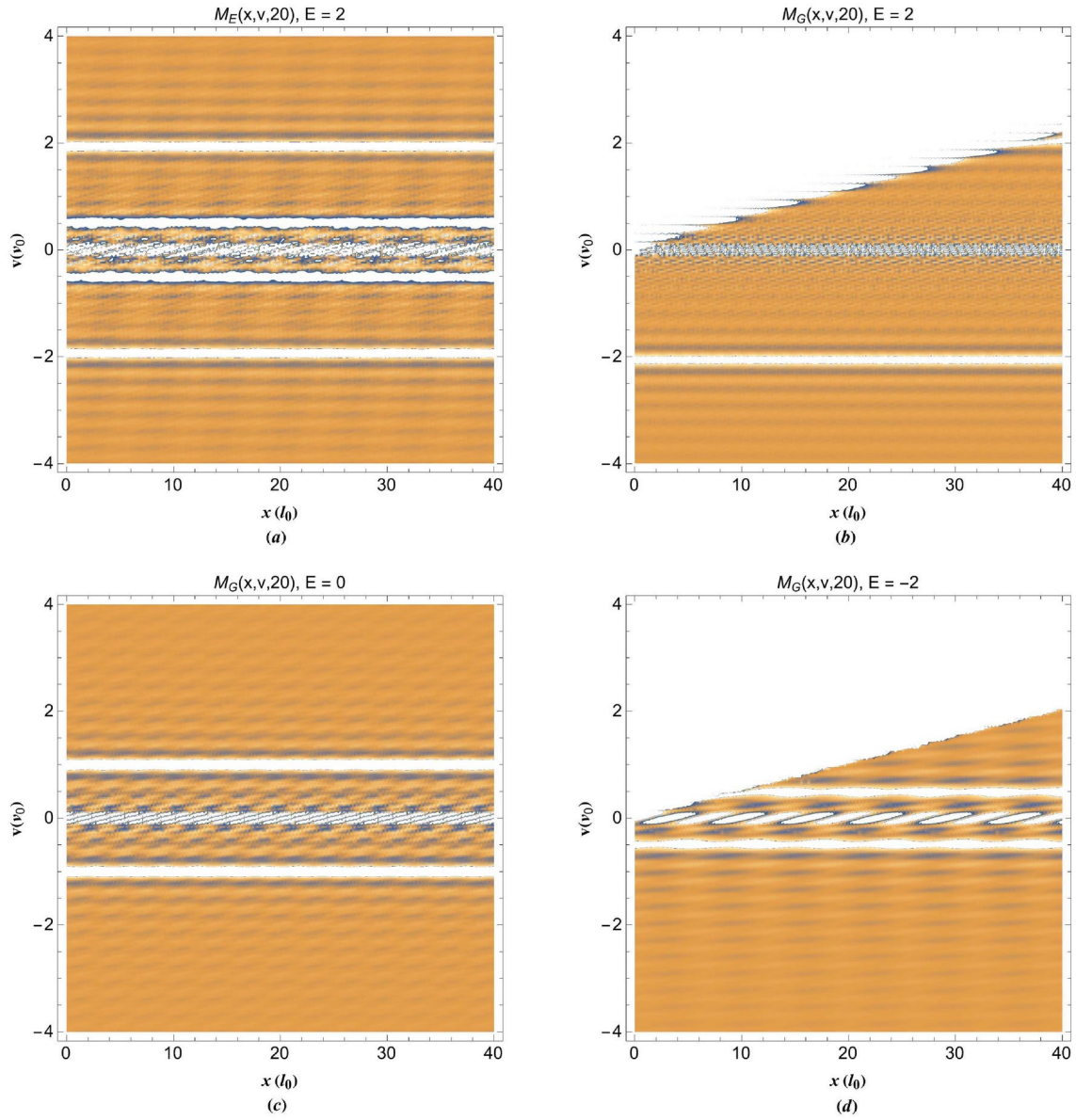

Fig. 9. (**a**) The modified Wigner function phase-space profile for plasmon excitation at orbital $E = 2$ at time $t = 20$. (**b**) The modified Wigner function phase-space profile for GQ excitation at orbital $E = 2$ at time $t = 20$. (**c**) The modified Wigner function phase-space profile for GQ excitation at orbital $E = 0$ at time $t = 20$. (**d**) The modified Wigner function phase-space profile for GQ excitation at orbital $E = -2$ at time $t = 20$.

$$k_c = \sqrt{\frac{1}{3}\left(\beta^{1/3} + \beta^{-1/3} - 1\right)}, \quad \beta = \frac{3\sqrt{3}}{2}\Gamma_G\sqrt{27\Gamma_G^2 - 4} + \frac{27\Gamma_G^2}{2} - 1, \tag{38}$$

where $\Gamma_G = 2E_J/mc^2$ contains three fundamental physical constants. While fundamental differences expected from dispersion relations of Ref.[72] and current model, it may be instructive to compare the critical Jeans wavenumber values obtained from these models in the nonrelativistic quantum regime. By the standard definition, the Jeans energy is $E_J = \hbar\omega_J$ with $\omega_J = \sqrt{4\pi G\rho_0}$ being the Jeans frequency and $v_J = \sqrt{2E_J/m}$ the corresponding Jeans speed. The quantum Jeans wavenumber is then the solution of the limiting non-relativistic matter wave energy dispersion relation, $\epsilon = \mu_0 + k^2/2 - 1/(2k^2) = 0$, in the normalized form which leads to the following dimensional equation $\hbar^2k^4/(4m^2) + \mu_0k^2/m - \omega_J^2 = 0$ in quasiparticle model resulting in $k_J = \left(2m/\hbar^2\right)^{1/2}\sqrt{\sqrt{\mu_0^2 + \hbar^2\omega_J^2} - \mu_0}$ in which μ_0 denotes the chemical potential. The Jeans wavenumber obtained from our model looks quite similar to the one obtained using equation Eq. (33) of Ref.[72] in the same limit, i.e., $k_J = \left(2m/\hbar^2\right)^{1/2}\sqrt{\sqrt{9m^2\langle u^2\rangle^2 + \hbar^2\omega_J^2} - 3m\langle u^2\rangle}$. They only differ in the term containing the average

speed arising from the statistical pressure. The results of the both models correctly reduce to the same value of $k_J = \sqrt{2mE_J}/\hbar$ in the absence of the statistical pressure. This comparison proves that the $E < 0$ quasiparticle band corresponds to the matter collapse in quantum regime quite analogous to the Jeans instability phenomenon. However, there no phenomenon associated with the positive energy band appear in previous models. Moreover, while there may be similarities of this kind in the results of the models, such a naive comparison of technical aspects of fundamentally different quantum kinetic, quantum hydrodynamic and the Lindhard response models which rely on single phase-speed (plane-wave) approximations with those of the dual phase-speed (dual plane-wave) quasiparticle model, based on the matter-wave energy dispersion, is not appropriate at all. This is because the quasiparticle's collective dispersion branch unlike that of the previous models diverges at the long-wavelength limit. Although the two models predict approximately that same value for the critical Jeans wavenumber, however, the calculations based on quantum hydrodynamic or wave-kinetic approaches add first-order quantum correction to classical dispersion relation beside the quantum statistical pressure effect and therefore still remain semiclassical. On the other hand, in the current quasiparticle model the gravitational field is quantized leading to quantized values of energy eigenvalues[59]. The later can have fundamental consequences for negative energies leading probably to bound state in the star or even black-hole formation, which needs further developments. Note that the key ingredient in current model which advances the previous ones is the introduction of a new de Broglie's wavelength which leads to quantization at the long wavelength limit and also its simple relation to the single particle excitations through the complementarity-like relation, $k_1 k_2 = i$.

As previously mentioned the dual lengthscale nature of quasiparticle theory of collective quantum excitations predicts results for effects such as the plasmon dispersion relation, the charge screening, the structure factor[68] and the phase-space structures[87] which are fundamentally different from those of Wigner-Poisson, quantum hydrodynamic and Lindhard dielectric based on random phase approximation. These differences are related to the quantization of the interaction field in current model via the electrostatic coupling of particle-like oscillations to the collective oscillations through a second de Broglie wavenumber, from one hand, and the self-consistent treatment of Wigner potential and avoiding the semiclassical expansion which leads to the violation of uncertainty principle, from the other. It is concluded that the Jeans instability result obtained in previous works[72–75] does not reflect the complete picture of gravitational excitations due to shortcoming in basic models used in the analysis, as discussed in Sec. II. However, current GQ model is a more general approach, which by considering a self-consistent treatment of Wigner potential[87], predicts three distinct regimes of expanding ($E > 0$), stable ($E = 0$) and collapsing ($E < 0$) matter under gravitational quantum interactions and clearly contains more information compared to previous models based on quantum hydrodynamic and wave-kinetic approaches[72–75] which account only for Jeans instability (collapsing in current analysis). This is because the previous models only capture the wave-like nature of quantum systems ($E < 0$ in current model) leaving-out the particle-like aspect due to semiclassical expansion of Wigner potential or function (considering the long wavelength limit), hence, fail to correctly account for dual lengthscale wave- and particle-like aspects in a unified picture. This may be compared to the similar case of the quantum charge screening[68] and failure of capturing the well-known Friedel oscillations in hydrodynamic approach which has led to inconsistent result with density functional and the Lindhard linear dielectric response theories[36] which fail to correctly capture the London-type dispersion, leading to an intense debate over the past decade[76–83].

Gravitational quasiparticle probability current

In this section, we obtain a generalized probability current density for GQ using the standard procedure. We start with linearized time-dependent Schrödinger-Poisson equation

$$2i\frac{\partial \mathcal{N}(\mathbf{r},t)}{\partial t} = -\Delta \mathcal{N}(\mathbf{r},t) + \Phi(\mathbf{r}) + \mu_0 \mathcal{N}(\mathbf{r},t), \tag{39a}$$

$$\Delta \Phi(\mathbf{r}) - \mathcal{N}(\mathbf{r},t) = 0. \tag{39b}$$

Note that Φ may contain a phase factor due to normalization. The continuity equation is

$$\nabla \cdot \mathbf{J}(\mathbf{r},t) = -\frac{\partial n}{\partial t} = -\frac{\partial \mathcal{N}(\mathbf{r},t)\mathcal{N}^*(\mathbf{r},t)}{\partial t} = -\mathcal{N}(\mathbf{r},t)\frac{\partial \mathcal{N}^*(\mathbf{r},t)}{\partial t} - \mathcal{N}^*(\mathbf{r},t)\frac{\partial \mathcal{N}(\mathbf{r},t)}{\partial t}. \tag{40}$$

Algebraic manipulation of time-dependent Schrödinger-Poisson equation leads to the following equations

$$2\mathcal{N}^*(\mathbf{r},t)\frac{\partial \mathcal{N}(\mathbf{r},t)}{\partial t} = i\mathcal{N}^*(\mathbf{r},t)\Delta \mathcal{N}(\mathbf{r},t) - i\mathcal{N}^*(\mathbf{r},t)\Phi(\mathbf{r}) - i\mu_0 \mathcal{N}^*(\mathbf{r},t)\mathcal{N}(\mathbf{r},t), \tag{41a}$$

$$2\mathcal{N}(\mathbf{r},t)\frac{\partial \mathcal{N}^*(\mathbf{r},t)}{\partial t} = -i\mathcal{N}(\mathbf{r},t)\Delta \mathcal{N}^*(\mathbf{r},t) + i\mathcal{N}(\mathbf{r},t)\Phi^* + i\mu_0 \mathcal{N}(\mathbf{r},t)\mathcal{N}^*(\mathbf{r},t). \tag{41b}$$

Combining the relations (40) and (41), we arrive at

$$2\nabla \cdot \mathbf{J}(\mathbf{r},t) = i\left[\mathcal{N}(\mathbf{r},t)\Delta \mathcal{N}^*(\mathbf{r},t) - \mathcal{N}^*(\mathbf{r},t)\Delta \mathcal{N}(\mathbf{r},t)\right] + i\left[\mathcal{N}^*(\mathbf{r},t)\Phi(\mathbf{r}) - \mathcal{N}(\mathbf{r},t)\Phi^*(\mathbf{r})\right]. \tag{42}$$

From Poisson's relation, we deduce

$$[\mathcal{N}^*(\mathbf{r},t)\Phi(\mathbf{r})-\mathcal{N}(\mathbf{r},t)\Phi^*(\mathbf{r})]=\Phi(\mathbf{r})\Delta\Phi^*(\mathbf{r})-\Phi^*(\mathbf{r})\Delta\Phi(\mathbf{r}),\tag{43}$$

which in combination with (40) leads to

$$2\nabla\cdot\mathbf{J}(\mathbf{r},t)=i\left[\mathcal{N}(\mathbf{r},t)\Delta\mathcal{N}^*(\mathbf{r},t)-\mathcal{N}^*(\mathbf{r},t)\Delta\mathcal{N}(\mathbf{r},t)\right]+i\left[\Phi(\mathbf{r})\Delta\Phi^*(\mathbf{r})-\Phi^*(\mathbf{r})\Delta\Phi(\mathbf{r})\right],\tag{44}$$

consequently resulting in the generalized form of probability current density

$$\mathbf{J}(\mathbf{r},t)=\frac{i}{2}\left[\mathcal{N}(\mathbf{r},t)\nabla\mathcal{N}^*(\mathbf{r},t)-\mathcal{N}^*(\mathbf{r},t)\nabla\mathcal{N}(\mathbf{r},t)\right]+\frac{i}{2}\left[\Phi(\mathbf{r})\nabla\Phi^*(\mathbf{r})-\Phi^*(\mathbf{r})\nabla\Phi(\mathbf{r})\right].\tag{45}$$

The time-independent probability current density is given as

$$\mathbf{J}_G(\mathbf{r})=\frac{i}{2}\left[\Psi(\mathbf{r})\nabla\Psi^*(\mathbf{r})-\Psi^*(\mathbf{r})\nabla\Psi(\mathbf{r})\right]+\frac{i}{2}\left[\Phi(\mathbf{r})\nabla\Phi^*(\mathbf{r})-\Phi^*(\mathbf{r})\nabla\Phi(\mathbf{r})\right].\tag{46}$$

A similar form can be obtained for electrostatic excitations as

$$\mathbf{J}_E(\mathbf{r})=\frac{i}{2}\left[\Psi(\mathbf{r})\nabla\Psi^*(\mathbf{r})-\Psi^*(\mathbf{r})\nabla\Psi(\mathbf{r})\right]-\frac{i}{2}\left[\Phi(\mathbf{r})\nabla\Phi^*(\mathbf{r})-\Phi^*(\mathbf{r})\nabla\Phi(\mathbf{r})\right].\tag{47}$$

Gravitational quasiparticle interference

Moreover, the generalized system of equations (39) (with plus/minus signs referring to electrostatic/gravitation case) admit a 3D time-independent solution of the form[61]

$$\begin{bmatrix}\Phi(r)\\ \Psi(r)\end{bmatrix}=\frac{Q}{2\alpha r}\begin{bmatrix}\Psi_0\mp k_2^2\Phi_0 & -\left(\Psi_0\mp k_1^2\Phi_0\right)\\ -\left(\Phi_0+k_1^2\Psi_0\right) & \Phi_0+k_2^2\Psi_0\end{bmatrix}\begin{pmatrix}e^{ik_1r}\\ e^{ik_2r}\end{pmatrix},\tag{48}$$

where Q is the corresponding pole (mass/charge) quantity and the characteristic wavenumbers are the same as for 1D excitations. Using the polar solution (48) in (46) and (47), we obtain

$$J_G(r)=\frac{\left(1+\sqrt{E^2+1}\right)k_2}{r^2\sqrt{E^2+1}},\quad J_E(r)=\frac{(1+E)(k_2-k_1)}{r^2\sqrt{E^2-1}}.\tag{49}$$

Note that the field-density probability currents give the correct dependence on r, since, $\nabla\cdot\mathbf{J}=0$ for stationary solutions. Note also that in the large value of energy $E\gg1$ both current densities reduce to the free particle value $J=k_2$ in normalized form. It can be easily checked that the conventional definition of probability current density based solely on the wavefunction, $\Psi(r)$ does not produce a consistent result. It is concluded that for an interacting gas of particles, the generalized relation for field-density probability current must be used. It is further noted that for a conserved number of particles N in the spherical volume, the relations $J_G=\rho_m v_G$ and $J_E=\rho_e v_E$ with $\rho_m\propto r^{-3}$ and $\rho_e\propto r^{-3}$ lead to the Hubble-like relations $v_G=H_G r$ and $v_E=H_E r$ in which the corresponding Hubble constants read

$$H_G=\frac{\left(1+\sqrt{E^2+1}\right)k_2}{\sqrt{E^2+1}},\quad H_E=\frac{(1+E)(k_2-k_1)}{\sqrt{E^2-1}}.\tag{50}$$

Figure 10 shows the energy dependence of probability current and Hubble's constant for both plasmon and GQ. Figure 10a shows the probability current density of plasmon. It is remarked that current density increases with the increase of quasiparticle energy. The current density of gravity quasiparticle excitations is depicted in Fig. 10b showing that the current density of negative energy GQs is relatively lower compared to those with positive ones. The same dependence on the quasiparticle energy is also present in the corresponding Hubble constants shown in Fig. 10c, d.Figure 11 shows the quasiparticle excitations in mono-polar forms with a unit central mass/charge at orbital. For electrostatic excitations the variations in both density and potential are dual-tone. It has been shown that the wave-particle interactions in electrostatic excitations lead to an oscillatory Lennard-Jones-type attractive potential around the central charge[68]. The mono-polar density-potential distributions are depicted in Fig. 11b for the same energy orbital. It is remarked that in this case, the wave-like oscillations are missing leading to a monotonic decrease of the density and fast oscillatory profile for potential around the central mass. The profiles for ground state GQ level $E=0$ are shown in Fig. 11c. In this case, while the density varies quite similar to the case in Fig. 11b, the potential oscillations are stronger with larger wavelengths. This effect is rather amplified for the negative energy-valued gravity excitations, shown in Fig. 11d.

The quasiparticle system, in the cartesian coordinate, has the following form

$$\frac{\partial^2\Psi(x,y,z)}{\partial x^2}+\frac{\partial^2\Psi(x,y,z)}{\partial y^2}+\frac{\partial^2\Psi(x,y,z)}{\partial z^2}\mp\Phi(x,y,z)=-2E\Psi(x,y,z),\tag{51a}$$

$$\frac{\partial^2\Phi(x,y,z)}{\partial x^2}+\frac{\partial^2\Phi(x,y,z)}{\partial y^2}+\frac{\partial^2\Phi(x,y,z)}{\partial z^2}-\Psi(x,y,z)=0,\tag{51b}$$

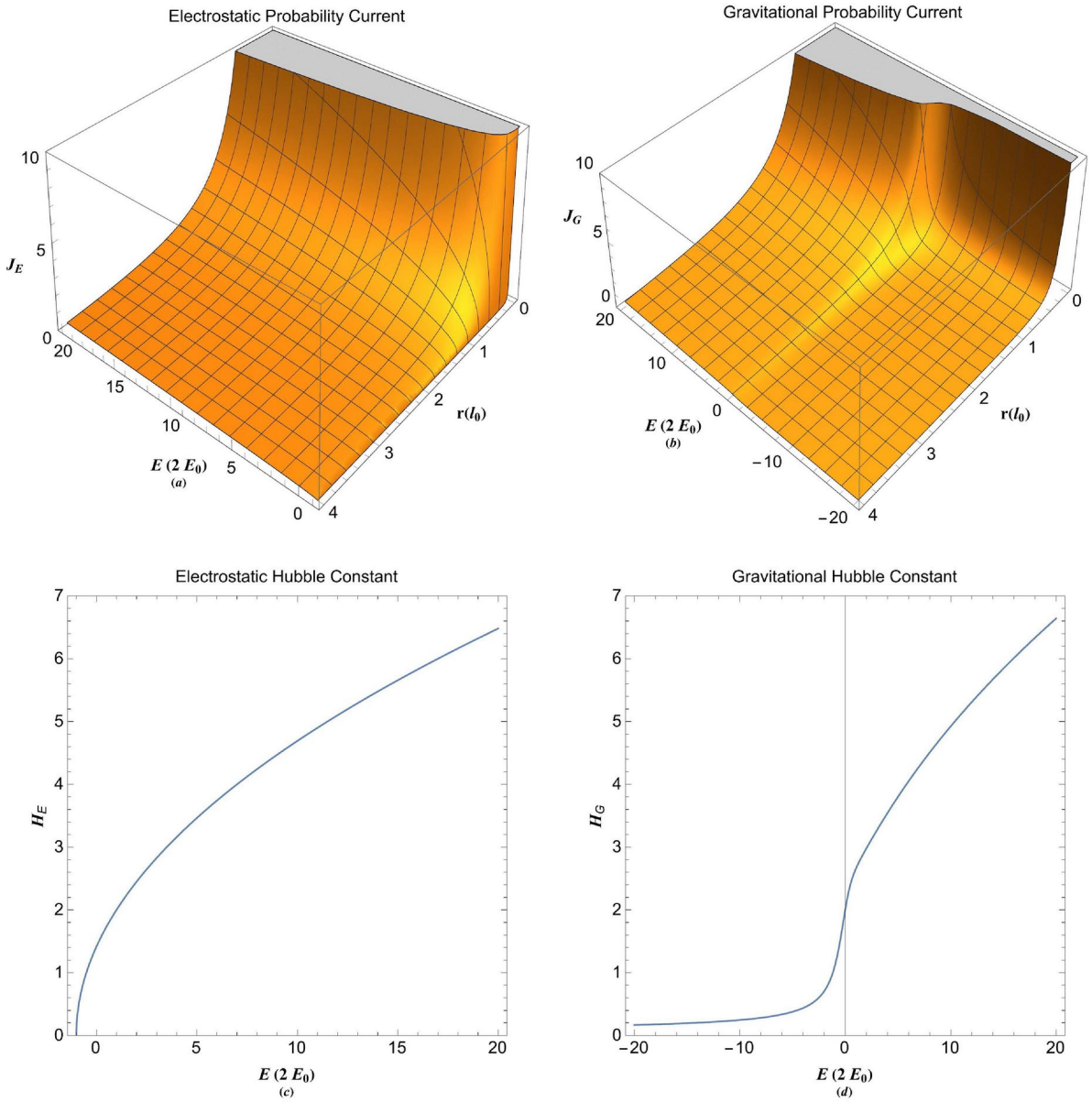

Fig. 10. (**a**) The probability current density of plasmon excitation as a function of quasiparticle energy and distance. (**b**) The probability current density of GQ excitation as a function of quasiparticle energy and distance. (**c**) The Hubble's constant of plasmon excitation as a function of quasiparticle energy. (**d**) The Hubble's constant of GQ excitation is a function of quasiparticle energy.

where $r=\sqrt{x^2+y^2+z^2}$ and the dipole(multipole) solution admits the following more general form[61]

$$\Phi=\frac{\left(1\mp k_2^2\right)\exp\left[ik_1\sqrt{(x-a)^2+y^2+z^2}\right]-\left(1\mp k_1^2\right)\exp\left[ik_2\sqrt{(x-a)^2+y^2+z^2}\right]}{2\alpha\sqrt{(x-a)^2+y^2+z^2}} \tag{52a}$$

$$+\frac{\left(1\mp k_2^2\right)\exp\left[ik_1\sqrt{(x+a)^2+y^2+z^2}\right]-\left(1\mp k_1^2\right)\exp\left[ik_2\sqrt{(x+a)^2+y^2+z^2}\right]}{2\alpha\sqrt{(x+a)^2+y^2+z^2}}, \tag{52b}$$

$$\Psi=\frac{\left(1+k_1^2\right)\exp\left[ik_2\sqrt{(x-a)^2+y^2+z^2}\right]-\left(1+k_2^2\right)\exp\left[ik_1\sqrt{(x-a)^2+y^2+z^2}\right]}{2\alpha\sqrt{(x-a)^2+y^2+z^2}} \tag{52c}$$

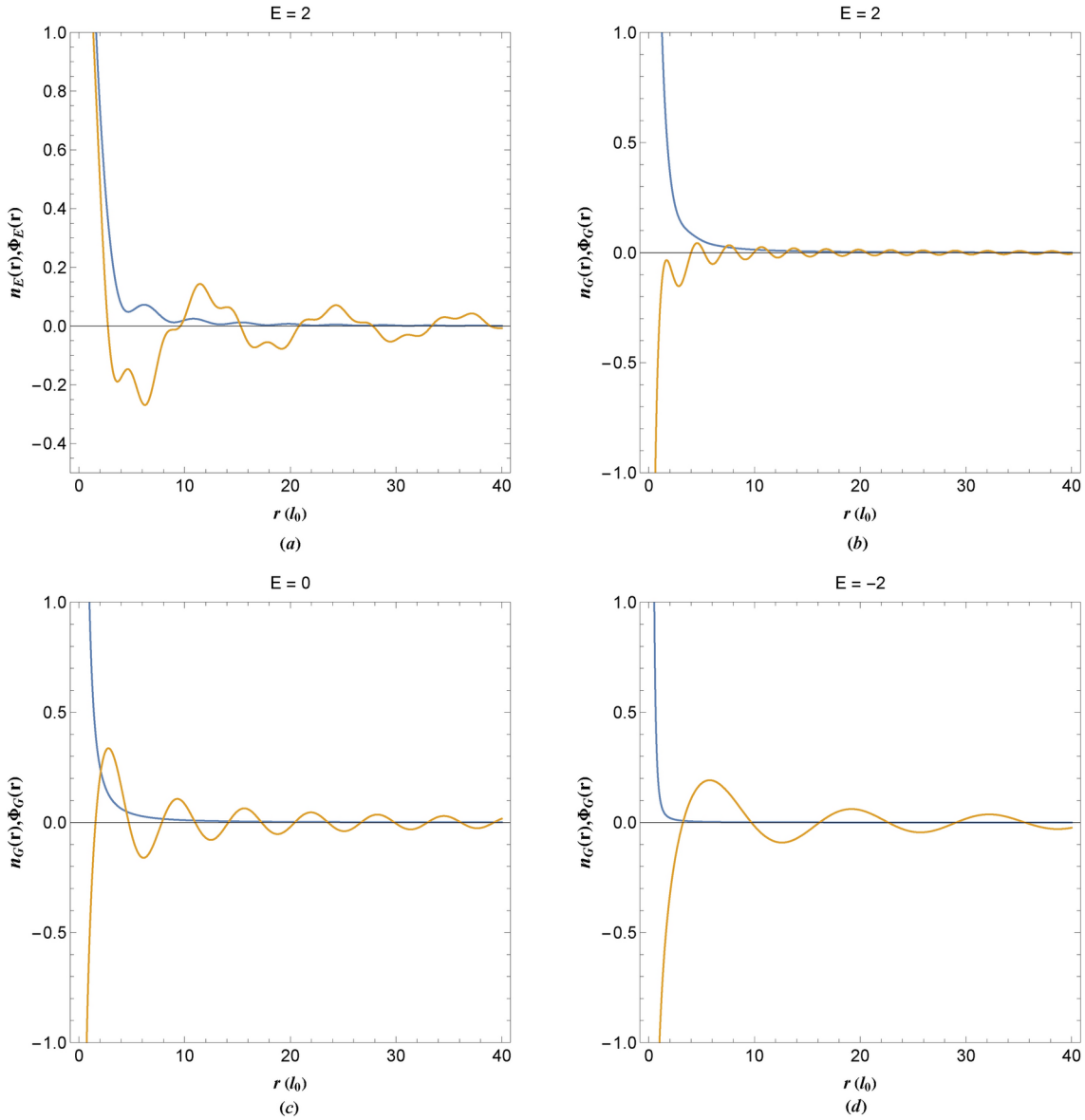

Fig. 11. (**a**) The radial density and electrostatic potential distribution of mono-pole plasmon excitation with unit charge at orbital $E = 2$. (**b**) The radial density and gravitational potential distribution of mono-pole GQ excitation with unit mass at orbital $E = 2$. (**c**) The radial density and gravitational potential distribution of mono-pole GQ excitation with unit mass at orbital $E = 0$. (**d**) The radial density and gravitational potential distribution of mono-pole GQ excitation with unit mass at orbital $E = -2$.

$$+\frac{\left(1+k_1^2\right)\exp\left[ik_2\sqrt{(x+a)^2+y^2+z^2}\right]-\left(1+k_2^2\right)\exp\left[ik_1\sqrt{(x+a)^2+y^2+z^2}\right]}{2\alpha\sqrt{(x+a)^2+y^2+z^2}}, \tag{52d}$$

where we have chosen $Q = 1$ and $\Phi_0 = \Psi_0 = 1$ and $\Phi_0' = \Psi_0' = 0$, for simplicity.

Figure 12 shows the bipolar density profiles using the solutions (52) for electrostatic and gravity excitations. Figure 12a shows the interference pattern forming around two charges of the same sign separated at distance $d = 2a$ at energy orbital $E = 2$. The formation of complex density structures around poles is due to quantum interference between wave-like and particle-like excitations in the electrostatic case. In the case of gravity excitations with positive energy value and the same dipole separation, the interference pattern is quite different due to wave-like damping of positive energy GQs. For the zero-energy orbital, the poles are isolated as compared to Fig. 12b whereas they are merged for negative energy orbital GQ, shown in Fig. 12d. The dissimilar profiles of these dipole GQ effects may be compared to related cosmological events.Figure 13 shows the stream plots of planar probability current density for electrostatic and gravitational dipole structures. The quantum trajectories correspond to the optimal mass/charge transport around the gravitational/electrostatic dipole. Figure 13a shows

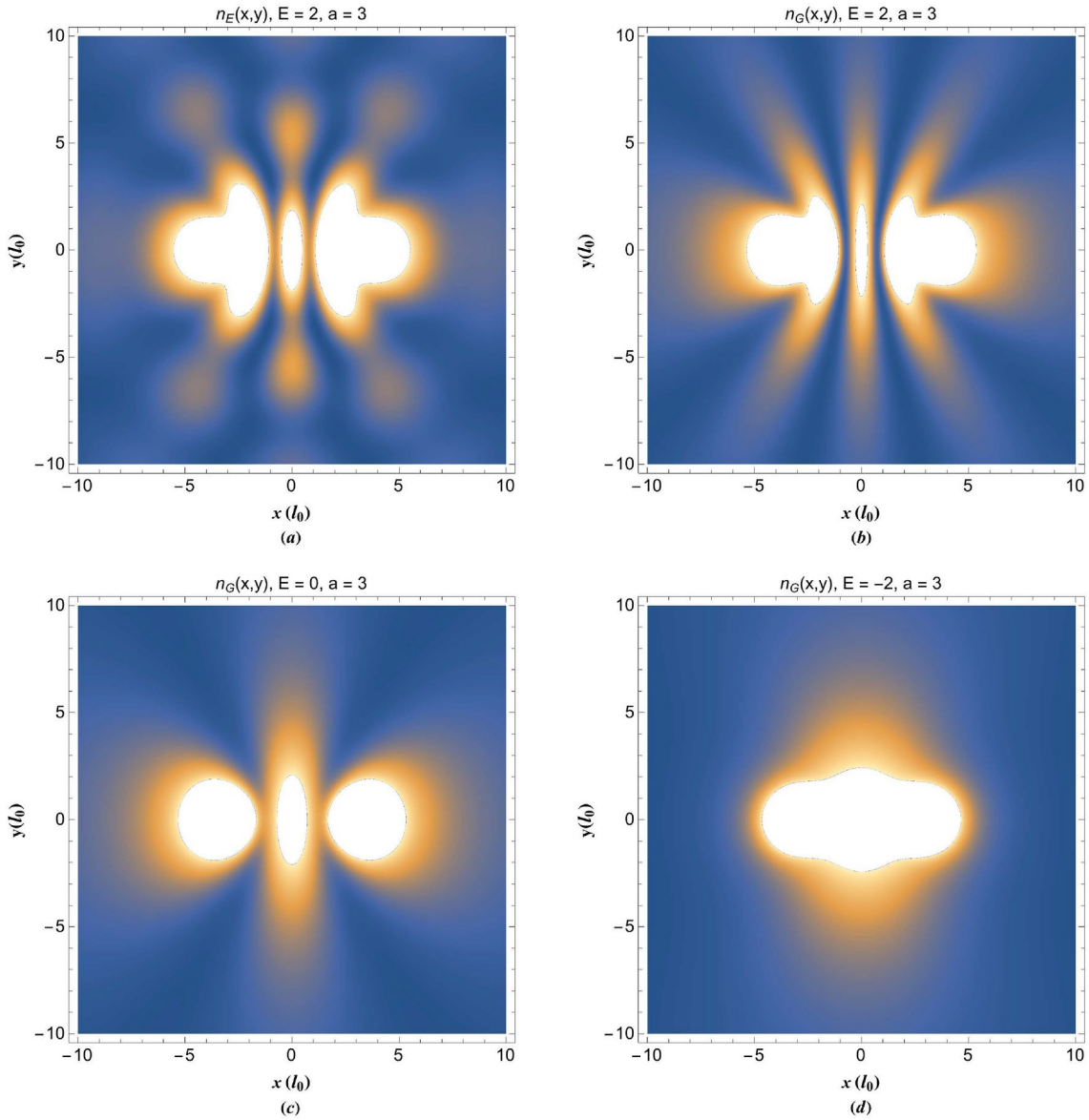

Fig. 12. (**a**) The unit charge electrostatic dipolar density distribution of plasmon excitation at energy orbital $E = 2$. (**b**) The unit mass gravitational dipolar density distribution of plasmon excitation at energy orbital $E = 2$. (**c**) The unit mass gravitational dipolar density distribution of plasmon excitation at energy orbital $E = 0$. (**d**) The unit mass gravitational dipolar density distribution of plasmon excitation at energy orbital $E = -2$.

the quantum back-flow effect (curved backward flow paths) arising due to the dual-tone nature of electrostatic excitations. The back-flow effect is absent for the gravitational excitations shown in Fig. 13b with similar parameter values as in Fig. 13a. However large distortions in the midway paths around the poles are still present. Figure 13c for ground state GQ orbital shows less distortions, however. The inflow mass trajectories of negative energy GQ are shown in Fig. 13d revealing many little curved paths around the gravity poles.

Conclusion

In this research, we studied the gravitational collective quantum excitations (GQ) in the framework of the quasiparticle excitation model where each particle is assumed to be and stream localized in momentum space rather than position space. These streams are then coupled through the effective Poisson's relation with local density defined through the single-particle wavefunctions. The similarities and differences between the plasmon and GQs were remarked through the nonrelativistic and relativistic matter-wave dispersion of these excitations. The phase space evolution of the modified Wigner function was investigated which revealed that GQs similar to plasmon excitations in the absence of external potential evolve similar to a classical system of interacting particles in the absence of external forces. It was shown that due to either the particle-like or wave-like damping nature of GQs, the phase space evolution of gravitational fluid leads to momentum spreading to positive values

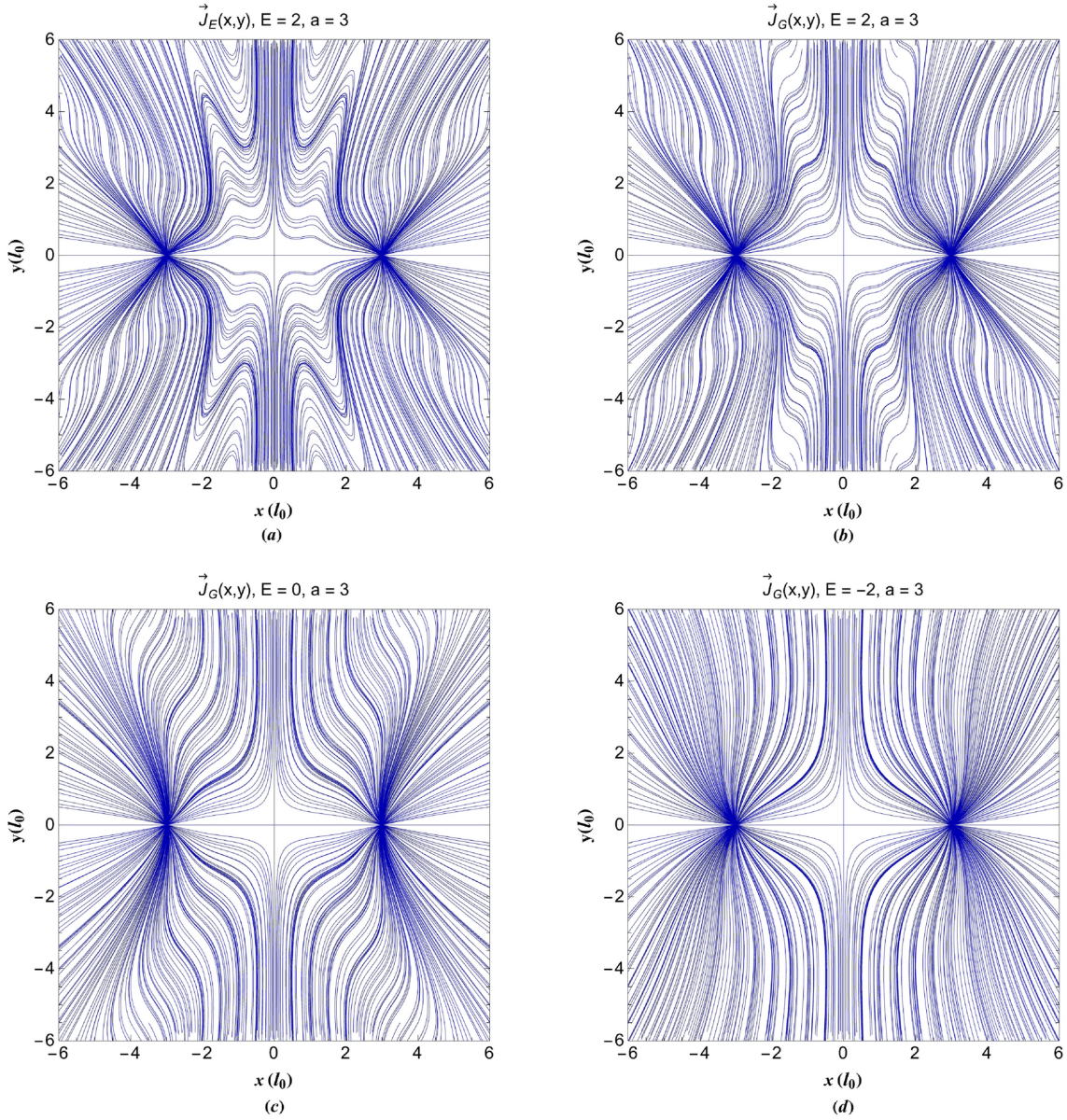

Fig. 13. (**a**) The unit charge electrostatic dipolar stream distribution of plasmon excitation at energy orbital $E = 2$. (**b**) The unit mass gravitational dipolar stream distribution of plasmon excitation at energy orbital $E = 2$. (**c**) The unit mass gravitational dipolar stream distribution of plasmon excitation at energy orbital $E = 0$. (**d**) The unit mass gravitational dipolar stream distribution of plasmon excitation at energy orbital $E = -2$.

as a consequence of quantum uncertainty, which is quite analogous to electron tunneling through the half-space confinement of electron gas. The generalized field-density probability current density relation was derived which leads to the Hubble-Lemaitre-like velocity law. The current study reveals some interesting peculiarities of GQs which can have fundamental applications in quantum cosmology.

Data availibility

The data that support the findings of this study are available from the corresponding author upon reasonable request.

Received: 24 January 2024; Accepted: 11 September 2024
Published online: 17 September 2024

References

1. Bernard, C. & Duncan, A. Regularization and renormalization of quantum field theory in curved space-time. *Annals Phys.* **107**, 201. https://doi.org/10.1016/0003-4916(77)90210-X (1977).

2. Arkani-Hamed, N., Dimopoulos, S. & Dvali, G. The hierarchy problem and new dimensions at a millimeter. *Phys. Lett. B* **429**, 263. https://doi.org/10.1016/S0370-2693(98)00466-3 (1998).
3. Aad, G. *et al*. Search for quantum black hole production in high-invariant-mass. *Phys. Rev. Lett*. **112** (9) 091804 (2006); https://doi.org/10.1103/PhysRevLett.112.091804
4. Randall, L. & Sundrum, R. An Alternative to Compactification. *Phys. Rev. Lett.* **83**, 4690. https://doi.org/10.1103/PhysRevLett.83.4690 (1999).
5. Randall, L. & Sundrum, R. Large mass hierarchy from a small extra dimension. *Phys. Rev. Lett.* **83**, 3370. https://doi.org/10.1103/PhysRevLett.83.3370 (1999).
6. Moskowitz, C. The cosmological constant is physics' most embarrassing problem. *Sci. Am*. **324**, 24 (2021).
7. Hubble, E. A relation between distance and radial velocity among extra-galactic nebulae. *PNAS* **15**, 168. https://doi.org/10.1073/pnas.15.3.168 (1929).
8. Anto, I. L. *et al*. Bayesian evidences for dark energy models in light of current observational data. *Phys. Rev. D* **97**, 043524. https://doi.org/10.1103/PhysRevD.97.043524 (2018).
9. Ellis, J. & Haghelin, J. S. Search for violations of quantum mechanics. *Nucl. Phys. B* **241**, 381 (1984).
10. Wang, C. H. T., Bingham, R. & Mendonca, J. T. Quantum gravitational decoherence of matter waves. *Class. Quantum Grav.* **23**, L59–L65. https://doi.org/10.1088/0264-9381/23/18/L01 (2006).
11. Huang, K. *Fundamental forces of nature: the story of gauge fields, Hackensack* (World Scientific, NJ, 2007).
12. Edward, W. Unravelling string theory. *Nature* **438**, 1085. https://doi.org/10.1038/4381085a (2005).
13. Lee, S. The trouble with physics: The rise of string theory, the fall of a science, and what comes next, New York: Houghton Mifflin Co. ISBN 978-0-618-55105-7 (2006).
14. Sabine, H. Experimental search for quantum gravity. In Frignanni, V. R. (ed.) Classical and quantum gravity: theory, analysis and applications. Nova Publishers. ISBN 978-1-61122-957-8 (2011).
15. Fermi, E. & Teller, E. The capture of negative mesotrons in matter. *Phys. Rev.* **72**, 399 (1947).
16. Bohm, D. & Pines, D. Coulomb interactions in a degenerate electron gas. *Phys. Rev.* **92**, 609 (1953).
17. Bohm, D. Avoiding negative probabilities in quantum mechanics. *Phys. Rev.* **85**, 166 (1952).
18. Bohm, D. A suggested interpretation of the quantum theory in terms of hidden variables. *Phys. Rev.* **85**, 180–193 (1952).
19. Pines, D. A collective description of electron interactions. *Phys. Rev.* **92**, 626 (1953).
20. Levine, P. & Roos, O. V. Plasma theory of the many-electron atom. *Phys. Rev.* **125**, 207 (1962).
21. Klimontovich, Y. & Silin, V. P. *Plasma Physics, edited by J* (E. Drummond, McGraw-Hill, New York, 1961).
22. Takabayasi, T. On the Formulation of Quantum Mechanics associated with Classical pictures. *Prog. Theor. Phys.* **8**, 143 (1952).
23. Takabayasi, T. Relativistic hydrodynamics of the dirac matter. Part I. General theory. *Prog. Theor. Phys.* **14**, 283 (1955).
24. Takabayasi, T. On the hydrodynamical representation of non-relativistic spinor equation. *Prog. Theor. Phys.* **12**, 810 (1954).
25. Takabayasi, T. On the separability of dirac equation. *Prog. Theor. Phys.* **9**, 681 (1953).
26. Takabayasi, T. Relativistic particle with internal rotational structure. *Nuovo. Cim.* **13**, 532 (1959).
27. Castro, C. & Zuazua, E. Flux identification for 1-d scalar conservation laws in the presence of shocks. *Math. Comp.* **1**, 38 (2006).
28. Castro, C. Nonlinear corrections to the Schrödinger equation from geometric quantum mechanics. *J. Math. Phys.* **31**, 2633 (1990).
29. Johna, D. L., Castro, L. C. & Pulfrey, D. L. Quantum capacitance in nanoscale device modeling. *J. Appl. Phys.* **96**, 5180 (2004).
30. Castro, C. On Weyl geometry, random processes, and geometric. *Found. Phys.* **80** (276), 2025 (2011).
31. Bohr, N. & Lindhard, J. Electron capture and loss by heavy ions penetrating through matter. *Dan. Mat. Fys. Medd.* **28**, 1 (1954).
32. Marklund, M., & Brodin, G. Dynamics of spin-$1/2$ quantum plasmas. *Phys. Rev. Lett.* **98**, 025001. https://doi.org/10.1103/PhysRevLett.98.025001 (2007).
33. Bonitz, M. et al. Theory and simulation of strong correlations in quantum Coulomb systems. *J. Phys. A* **36**, 5921 (2003).
34. Shukla, P. K. & Eliasson, B. Nonlinear aspects of quantum plasma physics. *Phys. Usp.* **53**, 76 (2010).
35. Stenflo, L. & Brodin, G. Large amplitude circularly polarized waves in quantum plasmas. *J. Phys. Plasmas* **76**, 261 (2010).
36. Akbari-Moghanjoughi, M. Hydrodynamic limit of Wigner-Poisson kinetic theory: Revisited. *Phys. Plasmas* **22**, 022103. *ibid.***22**, 039904 (E) (2015).
37. Shukla, P. K. & Eliasson, B. Nonlinear Interactions between Electromagnetic Waves and Electron Plasma Oscillations in Quantum Plasmas. *Phys. Rev. Lett.* **99**, 096401 (2007).
38. Stenflo, L. Resonant three-wave interactions in plasmas. *Phys. Scr.* **T50**, 15 (1994).
39. Shukla, P. K., Eliasson, B. & Stenflo, L. Stimulated scattering of electromagnetic waves carrying orbital angular momentum in quantum plasmas. *Phys. Rev. E* **86**, 016403 (2012).
40. Brodin, G. & Marklund, M. Spin magnetohydrodynamics. *New J. Phys.* **9**, 277 (2007).
41. Marklund, M. & Brodin, G. Dynamics of spin-$1/2$ quantum plasmas. *Phys. Rev. Lett.* **98**, 025001 (2007).
42. Moldabekov, Z., Tim Schoof, P., Ludwig, M. Bonitz. & Ramazanov, T. Statically screened ion potential and Bohm potential in a quantum plasma. *Phys. Plasmas* **22**, 102104. https://doi.org/10.1063/1.4932051 (2015).
43. Kim, H. M. & Jung, Y. D. Landau damping effects on collision-induced quantum interference in electron-hole plasmas. *EPL* **79**, 25001 (2007).
44. Miller, H. R. & Witta, P. J. *Active Galactic Nuclei* 202 (Springer-Verlag, Berlin, 1987).
45. Goldreich, P. & Julian, W. H. Pulsar electrodynamics. *Astrophys. J.* **157**, 869 (1969).
46. Michel, F. C. Theory of pulsar magnetospheres. *Rev. Mod. Phys.* **54**, 1 (1982).
47. Tandberg-Hansen, E. & Emshie, A. G. *The Physics of Solar Flares* 124 (Cambridge Univ. Press, Cambridge, 1988).
48. Rees, M. J. et al. (eds) *The Very Early Universe* (Cambridge Univ. Press, Cambridge, 1983).
49. Misner, W., Throne, K. S. & Wheeler, J. A. *Gravitation* 763 (Freeman, San Francisco, 1973).
50. Crouseilles, N., Hervieux, P. A. & Manfredi, G. Quantum hydrodynamic model for the nonlinear electron dynamics in thin metal films. *Phys. Rev. B* **78**, 155412 (2008).
51. Manfredi, G. & Haas, F. Self-consistent fluid model for a quantum electron gas. *Phys. Rev. B* **64**, 075316 (2001).
52. Diosi, L. Gravitation and quantummechanical localization of macroobjects. *Phys. Lett. A* **105**, 199 (1984).
53. Penrose, R. On gravity's role in quantum state reduction. *Gen. Rel. Gravity* **28**, 600 (1996).
54. Bahrami, Mohammad, Großardt, Andre, Donadi, Sandro & Bassi, Angelo. The Schrödinger-Newton equation and its foundations. *New J. Phys.* **16**, 115007. https://doi.org/10.1088/1367-2630/16/11/115007 (2014).
55. Padmanabhan, T. Obtaining the non-relativistic quantum mechanics from quantum field theory: Issues, folklores and facts. *Eur. Phys. J. C* **78**, 563. https://doi.org/10.1140/epjc/s10052-018-6039-y (2018).
56. Nuno, B. S. & Claudio, G. From quantum field theory to quantum mechanics. *Eur. Phys. J. C* **81**, 931. https://doi.org/10.1140/epjc/s10052-021-09742-0 (2021).
57. Sudarshan, E. C. G. The fundamental theorem on the relation between spin and statistics. *Proceedings of the Indian Academy of Sciences - Section A* **67**, 284. https://doi.org/10.1007/BF03049366 (1968).
58. Feynman, R. P., Robert, B., & Sands, M. L. The Feynman lectures on physics. **3** Addison-Wesley. ISBN 978-0-201-02118-9 (1965).
59. Akbari-Moghanjoughi, M. Quantized plasmon excitations of electron gas in potential well. *Phys. Plasmas* **26**, 012104. https://doi.org/10.1063/1.5078740 (2019).
60. Akbari-Moghanjoughi, M. Heat capacity and electrical conductivity of plasmon excitations. *Phys. Plasmas* **26**, 072106. https://doi.org/10.1063/1.5097144 (2019).

61. Akbari-Moghanjoughi, M. Quantum interference of three dimensional plasmon excitations. *Phys. Plasmas* **26**, 062105. https://doi.org/10.1063/1.5090366 (2019).
62. Akbari-Moghanjoughi, M. Energy band structure of multistream quantum electron system. *Sci. Rep.* **11**, 21099 (2021).
63. Akbari-Moghanjoughi, M. Effect of quantum charge screening on dual plasmon scattering. *Phys. Plasmas* **26**, 112102. https://doi.org/10.1063/1.5123621 (2019).
64. Akbari-Moghanjoughi, M. Quantum edge plasmon excitations and electron spill-out effect. *Phys. Plasmas* **29**, 082112. https://doi.org/10.1063/5.0102151 (2022).
65. Akbari-Moghanjoughi, M. Photo-plasmonic effect as the hot electron generation mechanism. *Sci. Rep.* **13**, 589. https://doi.org/10.1038/s41598-023-27775-1 (2023).
66. Akbari-Moghanjoughi, M. Collective quantum approach to resonant photo-plasmonic effect. *Phys. Plasmas* **30**, 082103. https://doi.org/10.1063/5.0159780 (2023).
67. Akbari-Moghanjoughi, M. *Phys. Plasmas* **28**, 082109. https://doi.org/10.1063/5.0057662 (2021).
68. Akbari-Moghanjoughi, M. Quasiparticle approach to collective quantum dielectric response. *Phys. Plasmas* **30**, 102109. https://doi.org/10.1063/5.0168275 (2023).
69. Akbari-Moghanjoughi, M. Effect of plasmon excitations in relativistic quantum electron gas. *Phys. Plasmas* **30**, 122101. https://doi.org/10.1063/5.0167561 (2023).
70. Sakharov, A. D. Vacuum quantum fluctuations in curved space and the theory of gravitation. *Sov. Phys. Usp.* **34**, 394. https://doi.org/10.1070/PU1991v034n05ABEH002498 (1991).
71. Verlinde, E. On the origin of gravity and the laws of Newton. *J. High En. Phys.* **4**, 29. https://doi.org/10.1007/jhep04(2011)029 (2011).
72. Mendonça, J. T. Wave-kinetic approach to the Schrödinger-Newton equation. *New J. Phys.* **21**, 023004 (2019).
73. Gomes, C. & Ourabah, K. Quantum kinetic theory of Jeans instability in non-minimal matter-curvature coupling gravity. *Eur. Phys. J. C* **83**, 40. https://doi.org/10.1140/epjc/s10052-023-11184-9 (2023).
74. Patidar, A. K., Joshi, H., Patidar, S., Pensia, R. K. & Mansuri, S. The effect of magnetized quantum plasma on jeans instability. *Zeitschrift für Naturforschung*[SPACE]https://doi.org/10.1515/zna-2023-0084 (2023).
75. Ourabah, K. On the collective properties of quantum media. *Eur. Phys. J. Plus* **138**, 55. https://doi.org/10.1140/epjp/s13360-022-03641-3 (2023).
76. Bonitz, M., Pehlke, E. & Schoof, T. Failure of linearized quantum hydrodynamics. *Phys. Rev. E* **87**, 033105 (2013).
77. Shukla, P. K., Eliasson, B. & Akbari-Moghanjoughi, M. Reply to "Comment on 'Attractive forces between ions in quantum plasmas: Failure of linearized quantum hydrodynamics'. *Phys. Rev. E* **87**, 037101 (2013).
78. Bonitz, M., Pehlke, E. & Schoof, T. Reply to Comment on 'Attractive forces between ions in quantum plasmas: Failure of linearized quantum hydrodynamics'. *Phys. Rev. E* **87**, 037102 (2013).
79. Shukla, P. K., Eliasson, B. & Akbari-Moghanjoughi, M. Discussion on Novel attractive force between ions in quantum plasmas–failure of simulations based on a density functional approach. *Phys. Scr.* **87**, 018202 (2013).
80. Bonitz, M., Pehlke, E. & Schoof, T. Discussion on 'Novel attractive force between ions in quantum plasmas—Failure of simulations based on a density functional approach. *Phys. Scr.* **88**, 057001 (2013).
81. Stanton, L. G., & Murillo, M. S. Unified description of linear screening in dense plasmas. *Phys. Rev. E* **91**, 033104 (2015); *ibid.* **91**, 049901 (E) (2015).
82. Michta, D., Graziani, F. & Bonitz, M. Quantum hydrodynamics for plasmas: A thomas-fermi theory perspective. *Contrib. Plasma Phys.* **55**, 437 (2015).
83. Moldabekov, Zh., Schoof, T., Ludwig, P., Bonitz, M. & Ramazanov, T. Statically screened ion potential and Bohm potential in a quantum plasma. *Phys. Plasmas* **22**, 102104 (2015).
84. vom Felde, A., Sprosser-Prou, J. & Fink, J. Valence-electron excitations in the alkali metals. *Phys. Rev. B* **40**, 10181 (1989).
85. Perepelkin, E. E. *et al*. Is the Moyal equation for the Wigner function a quantum analogue of the Liouville equation? *J. Stat. Mech.* 093102. https://doi.org/10.1088/1742-5468/acf8bd (2023).
86. Case, William B. Wigner functions and Weyl transforms for pedestrians. *Am. J. Phys.* **76**(10), 937. https://doi.org/10.1119/1.2957889 (2008).
87. Akbari-Moghanjoughi, M. Phase-space evolution of quasiparticle excitations in electron gas. *Phys. Plasmas* **31**, 032109. https://doi.org/10.1063/5.0194921 (2024).
88. Bonnor, W. B. Negative mass in general relativity. *Gen. Relat. Gravit.* **21**, 1143. https://doi.org/10.1007/BF00763458 (1989).
89. Farnes, J. S. A unifying theory of dark energy and dark matter: Negative masses and matter creation within a modified CDM framework. A &A **21**, A92 620. https://doi.org/10.1051/0004-6361/201832898 (2018).
90. Socas-Navarro, H. Can a negative-mass cosmology explain dark matter and dark energy? A &A, A5 626. https://doi.org/10.1051/0004-6361/201935317 (2019).
91. Bormashenko, E., Legchenkova, I. & Frenkel, M. Negative effective mass in plasmonic systems II: Elucidating the optical and acoustical branches of vibrations and the possibility of anti-resonance propagation. *Materials* **13**, 3512. https://doi.org/10.3390/ma13163512 (2020).
92. Mendonca, J. T. Wave kinetics of relativistic quantum plasmas. *Phys. Plasmas* **18**, 062101. https://doi.org/10.1063/1.3590865 (2011).
93. Wigner, E. On the quantum correction for thermodynamic equilibrium. *Phys. Rev.* **40**, 149 (1932).

Additional information

Correspondence and requests for materials should be addressed to M.A.-M.

Reprints and permissions information is available at www.nature.com/reprints.

Publisher's note Springer Nature remains neutral with regard to jurisdictional claims in published maps and institutional affiliations.